Collisions of light nuclei, Hot baryon matter

Elena Bratkovskaya

(GSI Darmstadt & Uni. Frankfurt)

Physics Program of the first stage of the NICA SPD experiment,

On-line

JINR, Dubna, Russia, 5-6 October 2020

Key questions of HICs at NICA energies:

The phase diagram of QCD

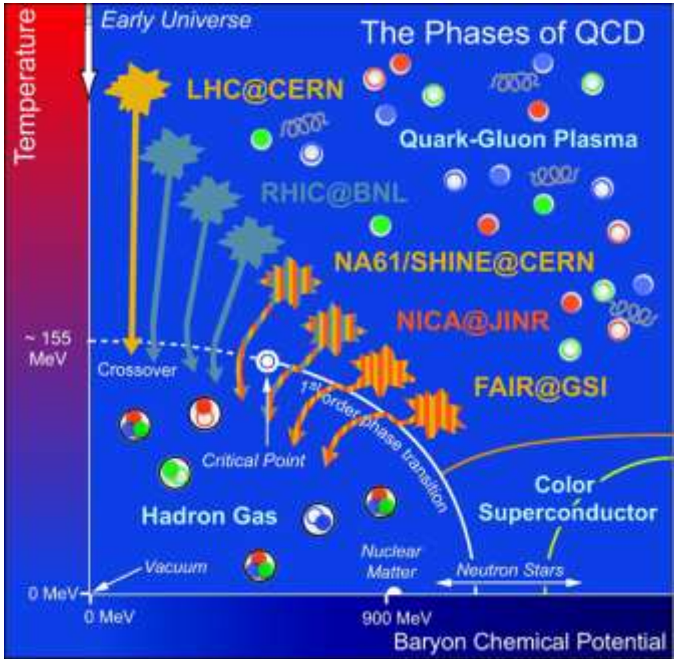

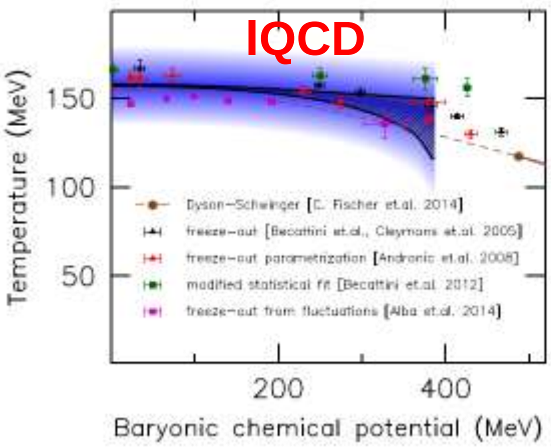

- What are the **properties of the hot and dense matter** created in HICs?
- What are **the degrees-of-freedom**, their properties and interactions?

QGP: strongly interacting liquid
→ non-perturbative QCD

Hadronic matter: higly compressed and hot medium
→ chiral symmetry restoration effects

Origin of the **phase transition**:
crossover → ? → 1st order?!

- **Strong electro-magnetic fields** are created during the HICs
→ polarization phenomena

NICA is located in a very interesting energy range !

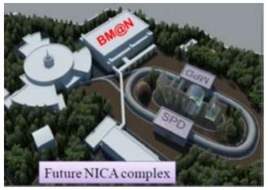

Experimental observables:

What are the experimental observables ?

‚Bulk‘ observables - multiplicities,
y-, p_T-spectra, flow coefficients v_n
Electromagnetic observables –
dileptons and photons
Clusters and hypernuclei production
Hard probes – open and hidden charm
....

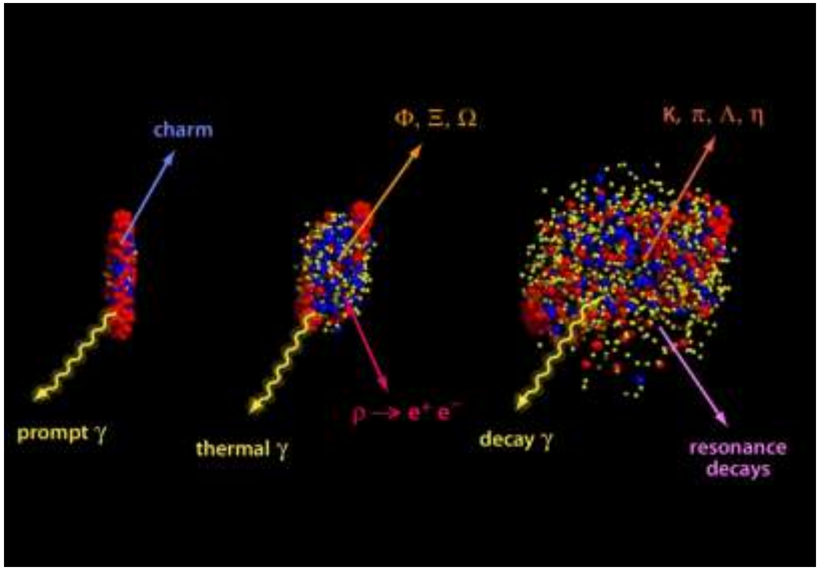

What are the systems to study ?

- **elementary pp and pn reactions:**
  of fundamental interests + provide a ‚reference frame‘ (i.e. input information) for the study of heavy-ion collisions
- **pA (and πA) reaction: cold nuclear matter effects**
- **light AA → heavy AA: many-body effects, isospin phenonena, EoS, critical point?**

Way to study:

Experimental energy scan of differential observables in order to find an ‚anomalous‘ behavior in comparison with theory

Dynamical description of heavy-ion collisions

The goal:
to study the properties of strongly interacting matter under extreme conditions from a microscopic point of view

Realization:
to develop a dynamical many-body transport approach
1) applicable for strongly interacting systems,
which includes:
2) phase transition from hadronic matter to QGP
3) chiral symmetry restoration

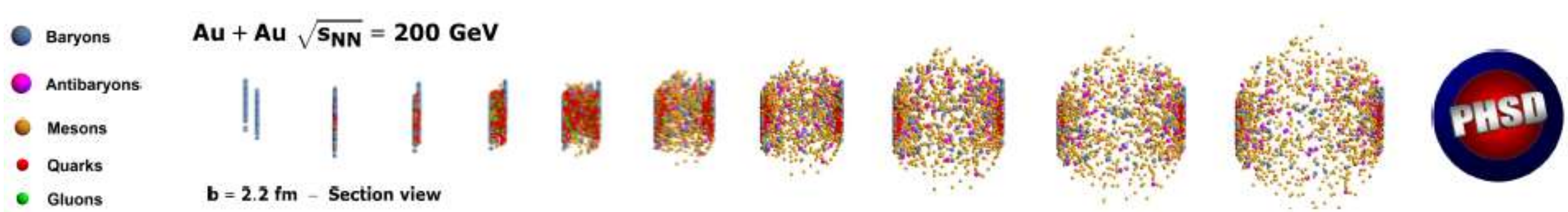

Degrees-of-freedom of QGP

For the microscopic transport description of the system one **needs to know all degrees of freedom** as well as their properties and interactions!

❖ lQCD gives QGP EoS at finite μ_B

! need to be interpreted in terms of degrees-of-freedom

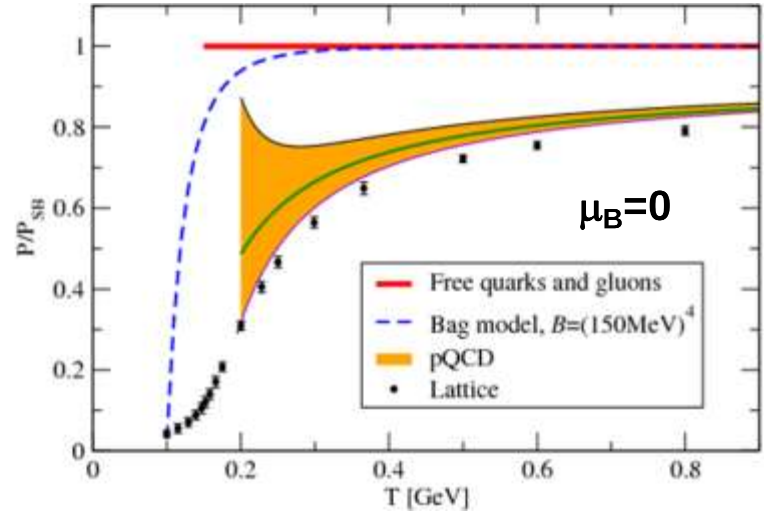

Non-perturbative QCD ← pQCD

pQCD:

- weakly interacting system
- massless quarks and gluons

Thermal QCD
= QCD at high parton densities:

- strongly interacting system
- massive quarks and gluons

➔ quasiparticles
= effective degrees-of-freedom

How to learn about the degrees-of-freedom of QGP from HIC?
➔ microscopic transport approaches
➔ comparison to HIC experiments

Dynamical QuasiParticle Model (DQPM)

DQPM – effective model for the description of **non-perturbative** (strongly interacting) QCD based on **lQCD EoS**

Degrees-of-freedom: strongly interacting **dynamical quasiparticles** - quarks and gluons

Theoretical basis :

- ❑ ‚resummed' single-particle Green's functions ➔ quark (gluon) propagator (2PI) : $G_q^{-1} = P^2 - \Sigma_q$

Properties of the quasiparticles are specified by scalar **complex self-energies:** $\Sigma_q = M_q^2 - i2\gamma_q\omega$

$Re\Sigma_q$: **thermal masses** (M_g, M_q); $Im\Sigma_q$: **interaction widths** (γ_g, γ_q) → spectral functions $\rho_q = -2ImG_q$

- ❑ introduce an **ansatz** (HTL; with few parameters) for the (T, μ_B) dependence of masses/widths
- ❑ evaluate the **QGP thermodynamics** in equilibrium using the Kadanoff-Baym theory
- ❑ fix DQPM parameters by comparison to the entropy density s, pressure P, energy density ε from DQPM to **lQCD** at μ_B =0

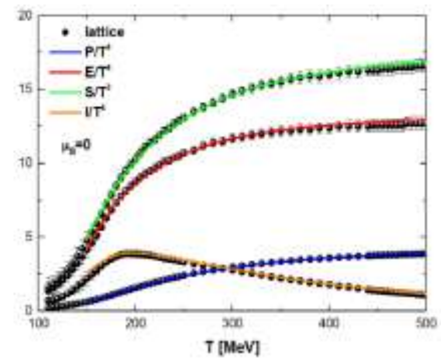

➔ Quasi-particle properties at (T, μ_B) :

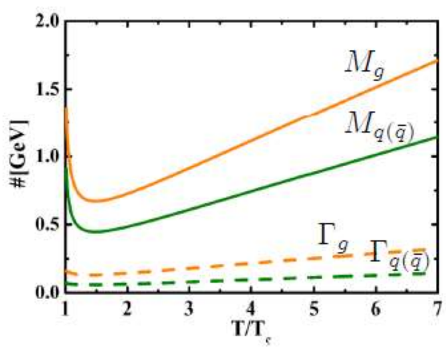

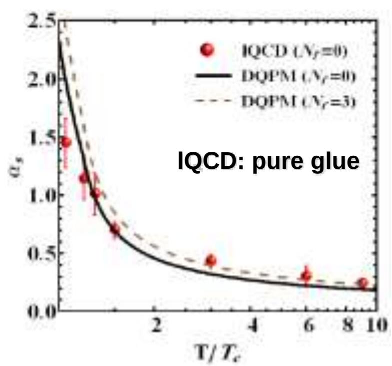

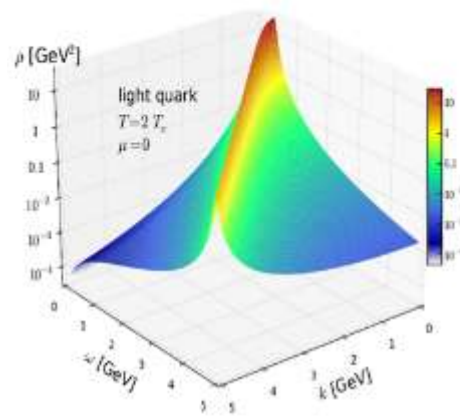

• **DQPM** provides **mean-fields** (1PI) for q,g and **effective 2-body partonic interactions** (2PI); gives **transition rates** for the formation of **hadrons** → **QGP in PHSD**

A. Peshier, W. Cassing, PRL 94 (2005) 172301; W. Cassing, NPA 791 (2007) 365: NPA 793 (2007), H. Berrehrah et al, Int.J.Mod.Phys. E25 (2016) 1642003; P. Moreau et al., PRC100 (2019) 014911; O. Soloveva et al., PRC101 (2020) 045203

Parton-Hadron-String-Dynamics (PHSD)

PHSD is a **non-equilibrium microscopic transport approach** for the description of **strongly-interacting hadronic and partonic matter** created in heavy-ion collisions

Dynamics: based on the solution of **generalized off-shell transport equations** derived from Kadanoff-Baym many-body theory

Initial A+A collision

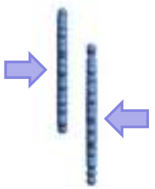

Partonic phase

Hadronization

Hadronic phase

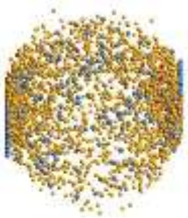

P.Moreau

- **Initial A+A collisions** :
  N+N → string formation → decay to pre-hadrons + leading hadrons

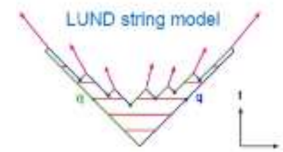

- **Formation of QGP stage** if local $\varepsilon > \varepsilon_{critical}$ =0.5 GeV/fm^3:
  dissolution of pre-hadrons → partons

- **Partonic phase - QGP:**
  QGP is described by the Dynamical QuasiParticle Model (DQPM) matched to reproduce lattice QCD EoS for finite T and μ_B (crossover)

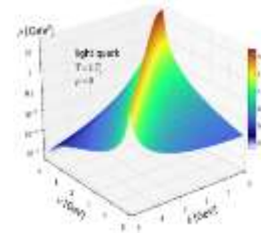

  - Degrees-of-freedom: strongly interacting quasiparticles: massive quarks and gluons (g,q,q_{bar}) with sizeable collisional widths in a self-generated mean-field potential

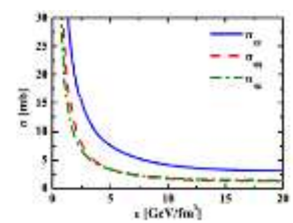

  - Interactions: (quasi-)elastic and inelastic collisions of partons

- **Hadronization** to colorless off-shell mesons and baryons:
  Strict 4-momentum and quantum number conservation

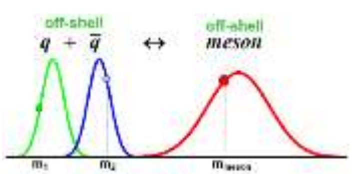

- **Hadronic phase:** hadron-hadron interactions – off-shell HSD

W. Cassing, E. Bratkovskaya, PRC 78 (2008) 034919; NPA831 (2009) 215; W. Cassing, EPJ ST 168 (2009) 3

Non-equilibrium dynamics: description of A+A with PHSD

❑ PHSD: highlights

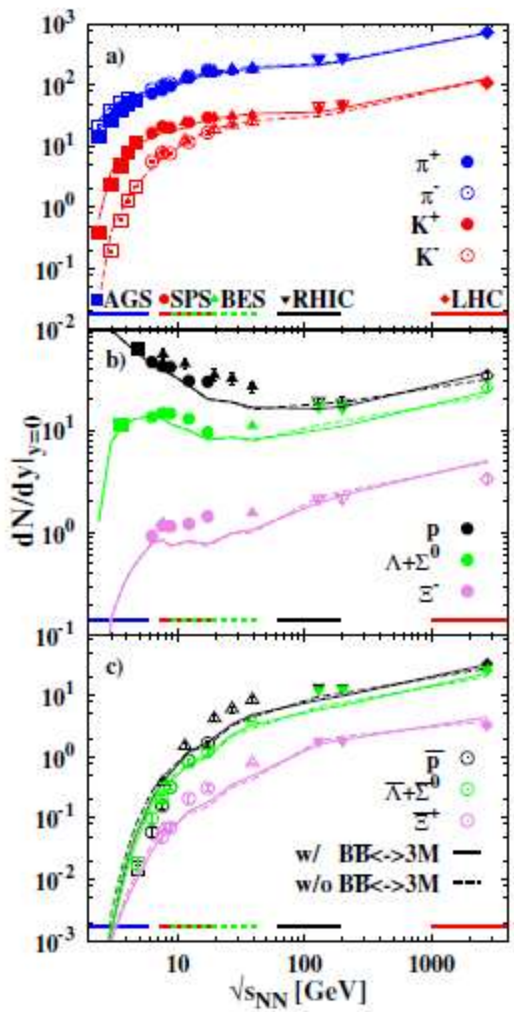

arXiv:1801.07557

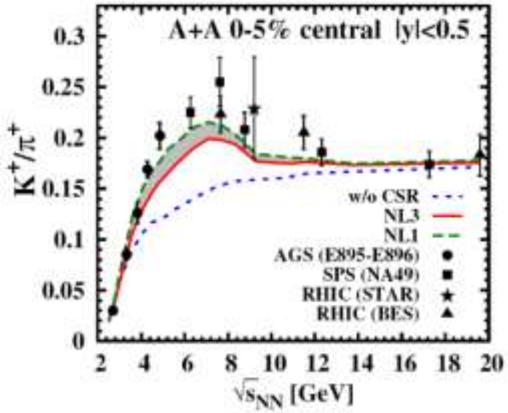

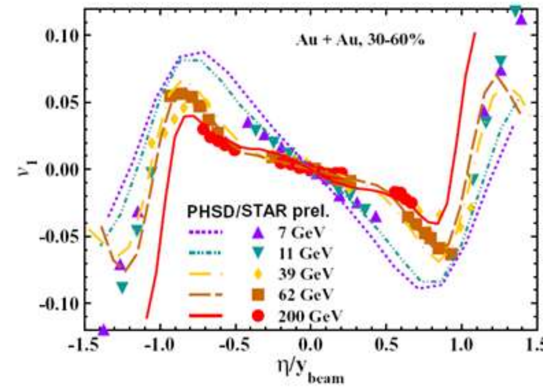

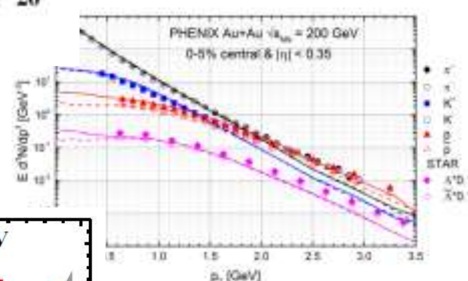

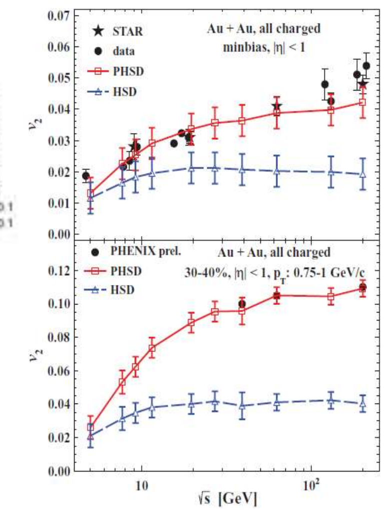

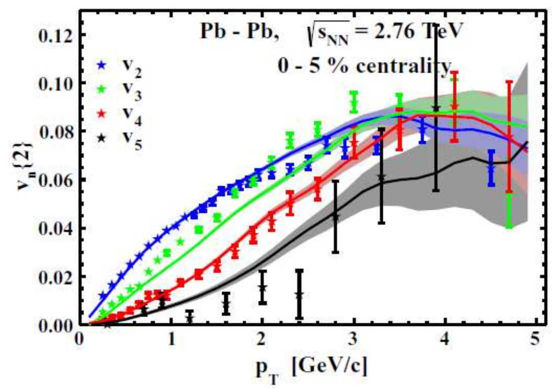

PRC 85 (2012) 011902; JPG42 (2015) 055106

❑ **PHSD** provides a **good description of ‚bulk' observables** (y-, p_T-distributions, flow coefficients v_n, …) from SIS to LHC

Traces of the QGP in observables in high energy heavy-ion collisions

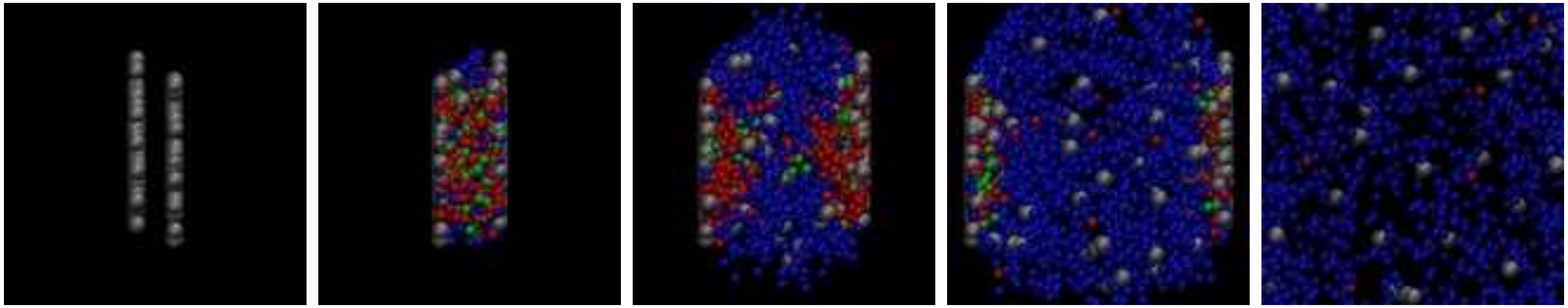

Partonic energy fraction in central A+A

Time evolution of the partonic energy fraction vs energy

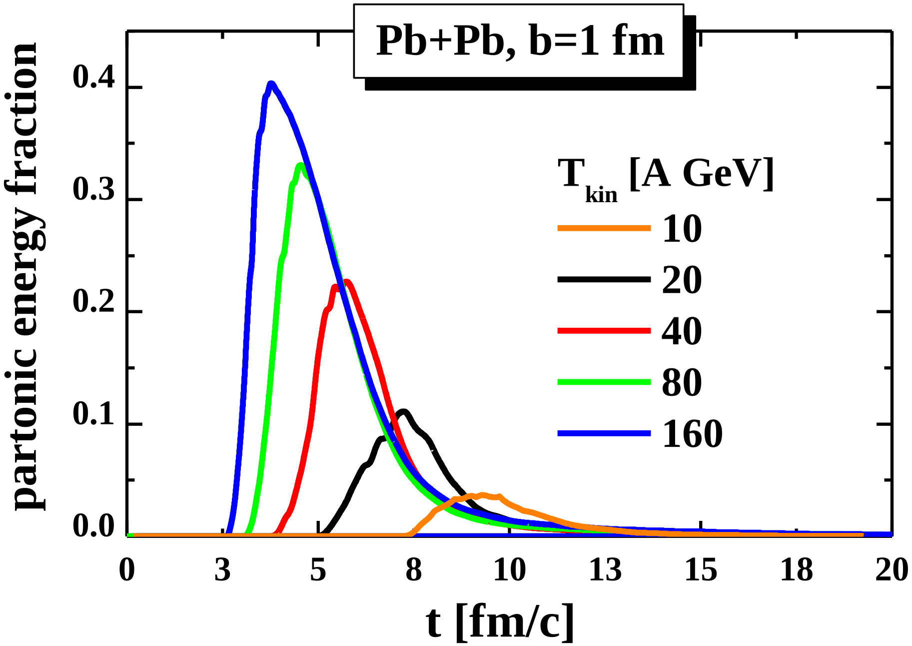

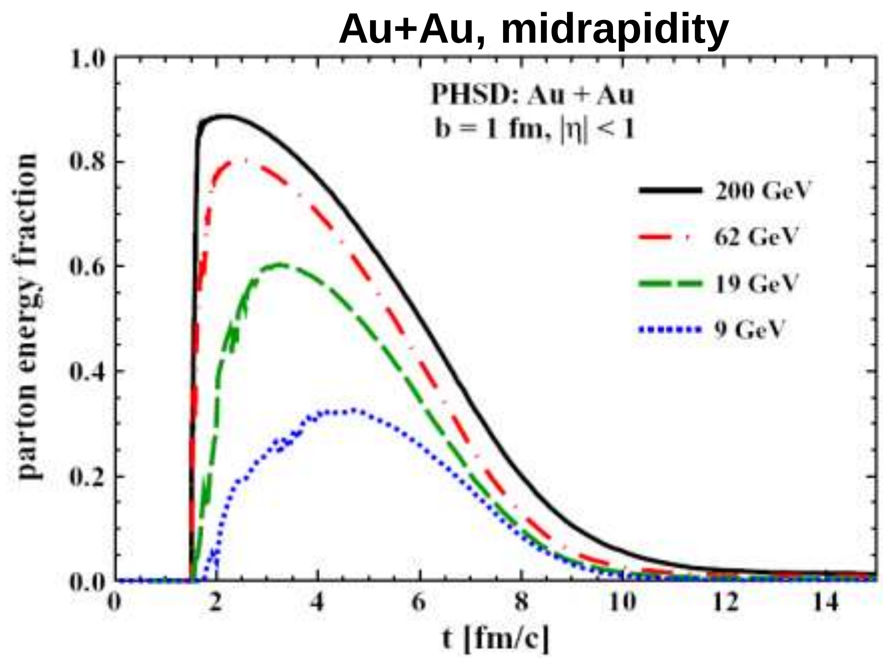

- Strong increase of partonic phase with energy from AGS to RHIC

- SPS: Pb+Pb, 160 A GeV: only about 40% of the converted energy goes to partons; the rest is contained in the large hadronic corona and leading partons
- RHIC: Au+Au, 21.3 A TeV: up to 90% - QGP

W. Cassing & E. Bratkovskaya, NPA 831 (2009) 215
V. Konchakovski et al., Phys. Rev. C 85 (2012) 011902

Transverse mass spectra from SPS to RHIC

Central Pb + Pb at SPS energies

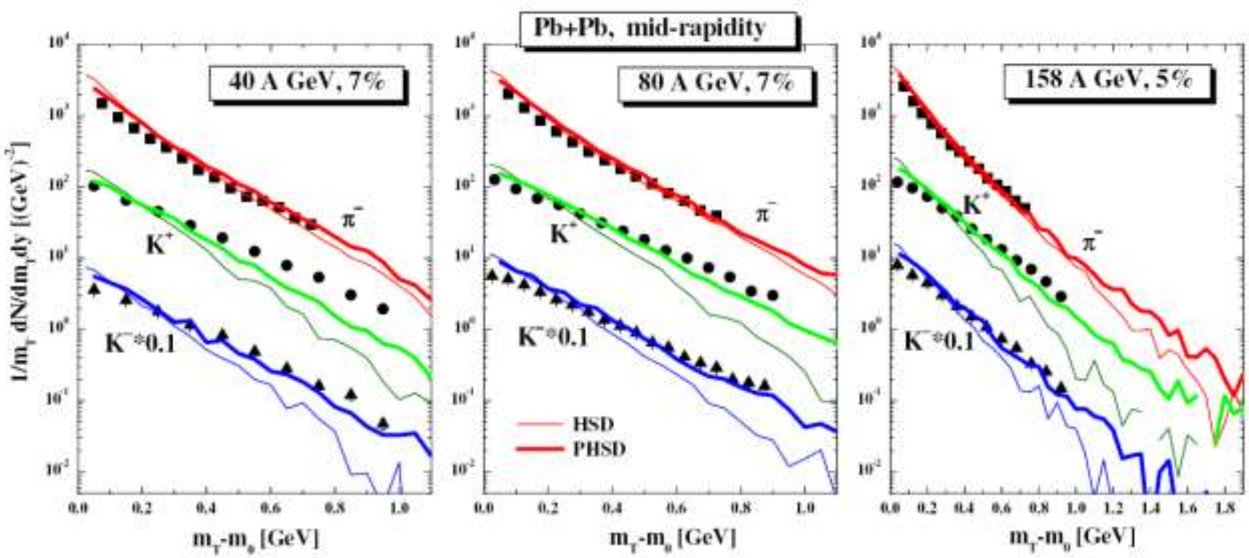

Central Au+Au at RHIC

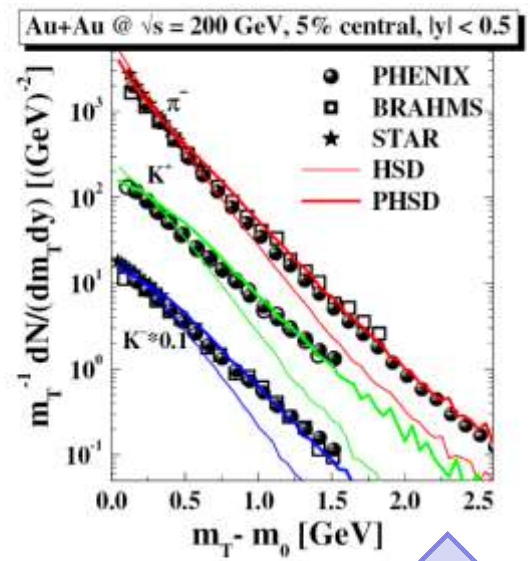

- PHSD gives harder m_T spectra and works better than HSD (wo QGP) at high energies – RHIC, SPS (and top FAIR, NICA)
- however, at low SPS (and low FAIR, NICA) energies the effect of the partonic phase decreases due to the decrease of the partonic fraction

W. Cassing & E. Bratkovskaya, NPA 831 (2009) 215
E. Bratkovskaya, W. Cassing, V. Konchakovski, O. Linnyk, NPA856 (2011) 162

PHSD: elliptic flow v_2

QGP: close to an ideal liquid
➔ strongly-interacting matter

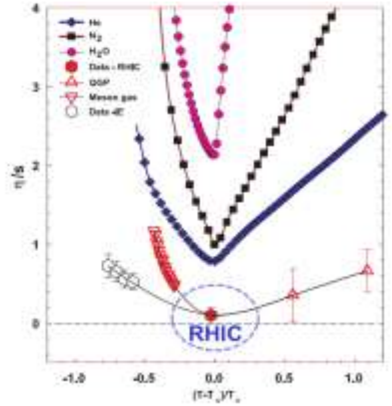

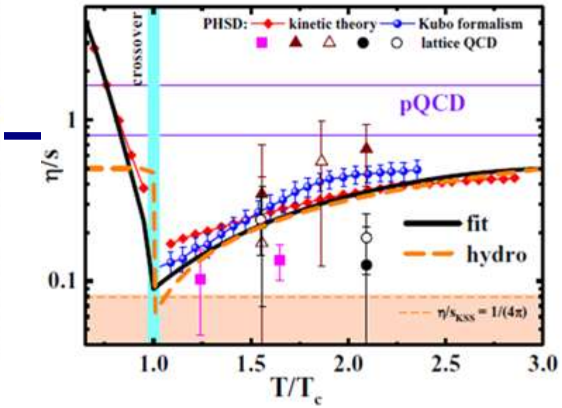

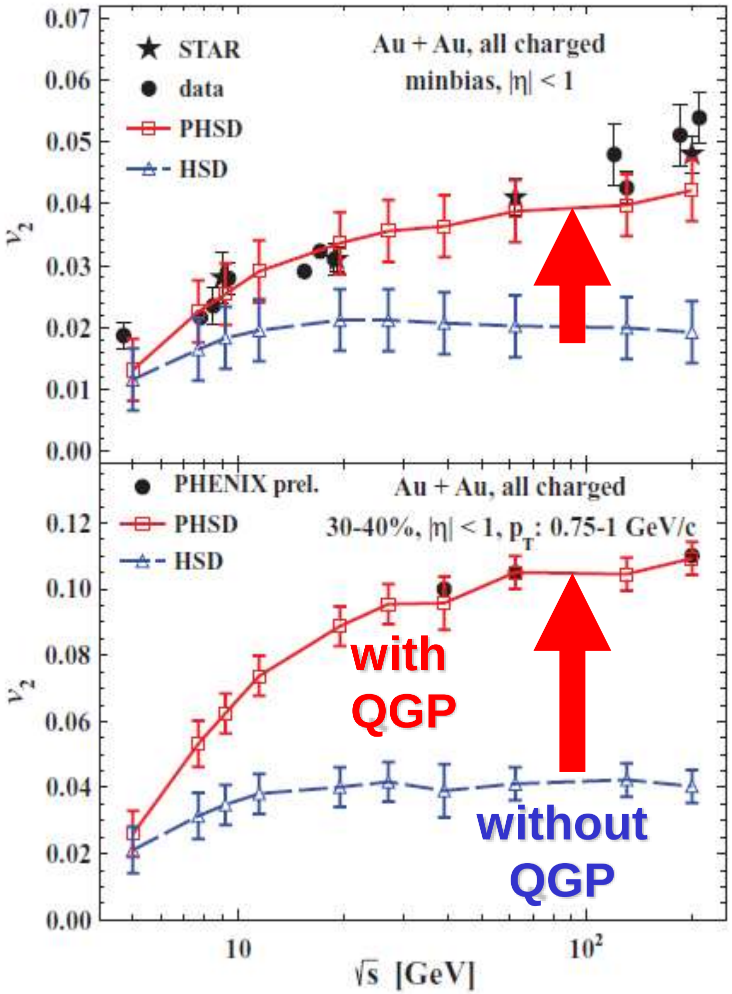

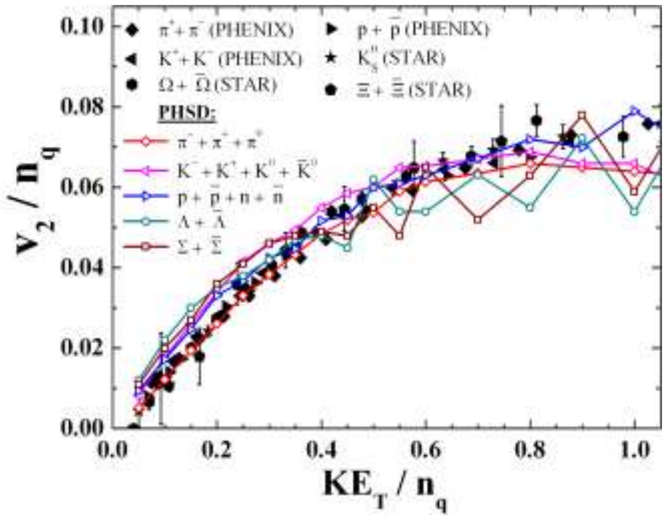

V. Konchakovski, E. Bratkovskaya, W. Cassing, V. Toneev, V. Voronyuk, PRC 85 (2012) 011902

- **Collectivity in QGP: scaling of v_2 with the number of constituent quarks n_q**
- **v_2 in PHSD is larger than in HSD due to the partonic interaction + repulsive scalar mean-field potential $U_s(\rho)$ for partons**
- **v_2 grows with bombarding energy due to the increase of the parton fraction**

Results for v_1 for HICs ($\sqrt{s_{NN}} = 27$ GeV)

- Exploring the partonic phase at finite chemical potential within the PHSD

v_1

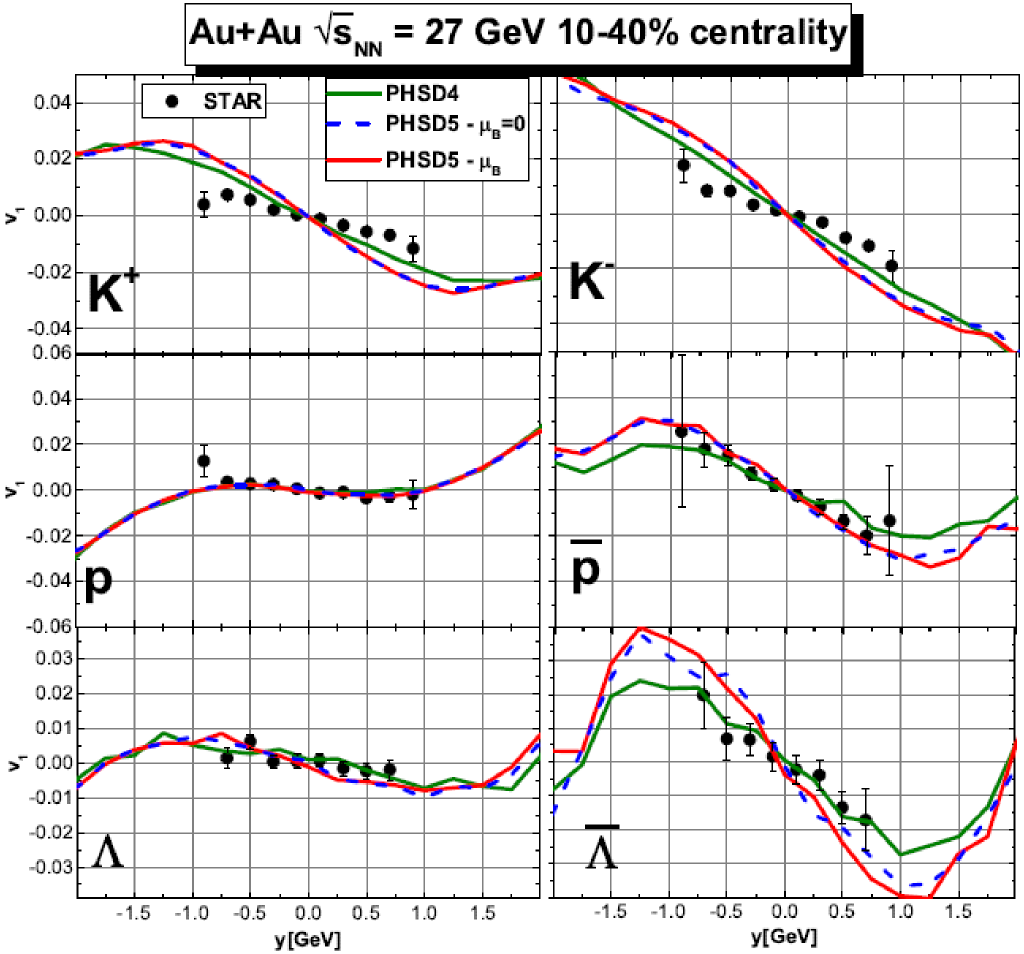

Messages from v_1, v_2 analysis within the PHSD 5.0:

- **weak dependence** of v_1, v_2 on μ_B
- **small influence** on v_1, v_2 of explicit $\sqrt{s}$ **-dependence** of total partonic cross sections σ + **angular dependence** of $d\sigma/d\cos\theta$ due to the relatively **small QGP volume**
- strong **flavor dependence** of v_1, v_2

O. Soloveva et al., arXiv:2001.07951, MDPI Particles 2020, 3, 178

V_n (n=2,3,4,5) of charged particles from PHSD at LHC

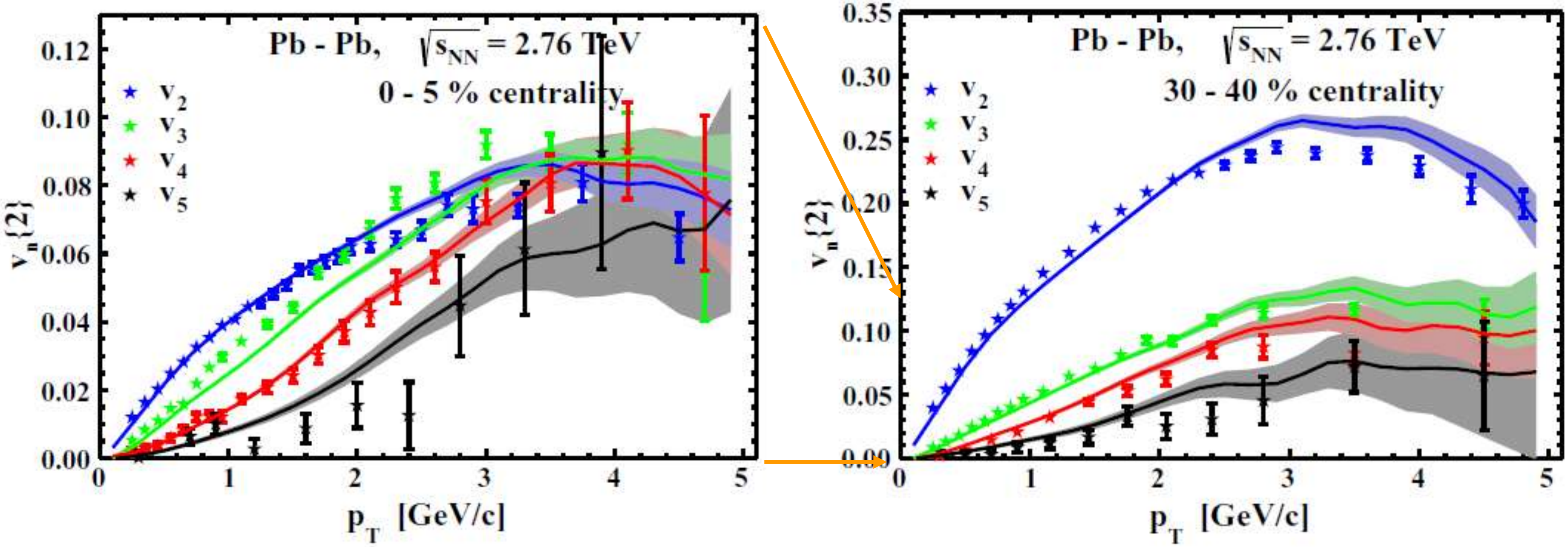

- PHSD: increase of v_n (n=2,3,4,5) with p_T
- v_2 increases with decreasing centrality
- v_n (n=3,4,5) show weak centrality dependence

symbols – ALICE PRL 107 (2011) 032301

lines – PHSD (e-by-e)

v_n (n=3,4,5) develops by interactions in the QGP and in the final hadronic phase

V. Konchakovski, W. Cassing, V. Toneev, J. Phys. G: Nucl. Part. Phys 42 (2015) 055106

Small colliding systems

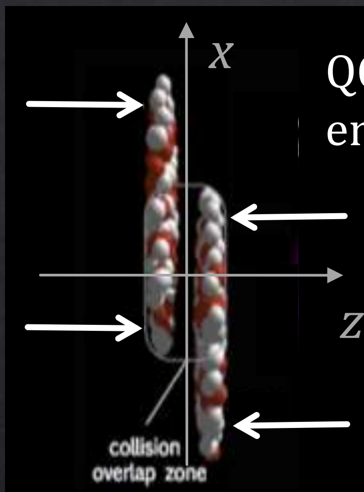

QGP initially expected only in high energy collisions of two heavy ions

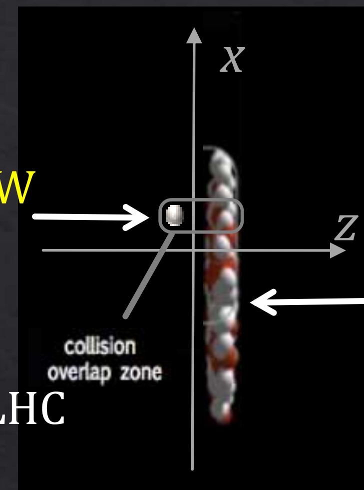

SIGNATURES OF COLLECTIVE FLOW FOUND IN SMALL SYSTEMS

in high-multiplicity events of

p/d/^{3}He+Au at RHIC, p+p, p+Pb at LHC

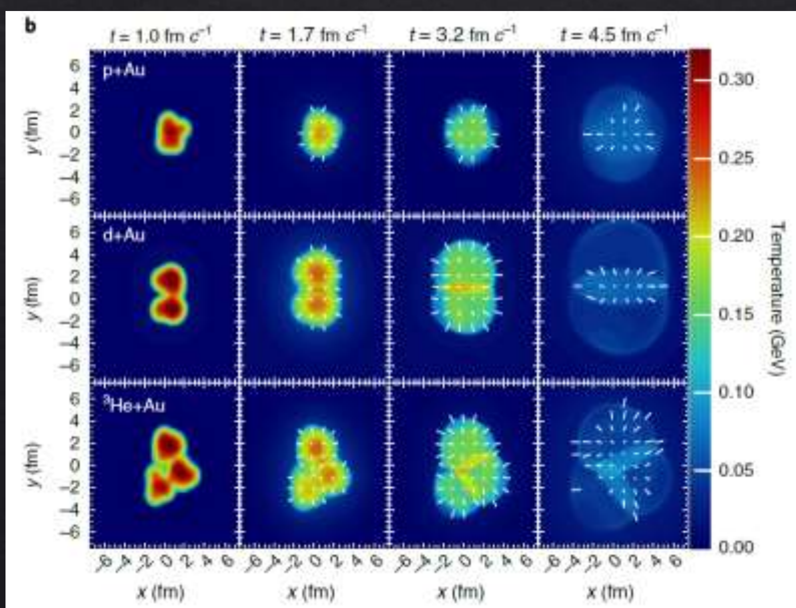

PHENIX Coll., Nature Phys. 15 (2019) 214

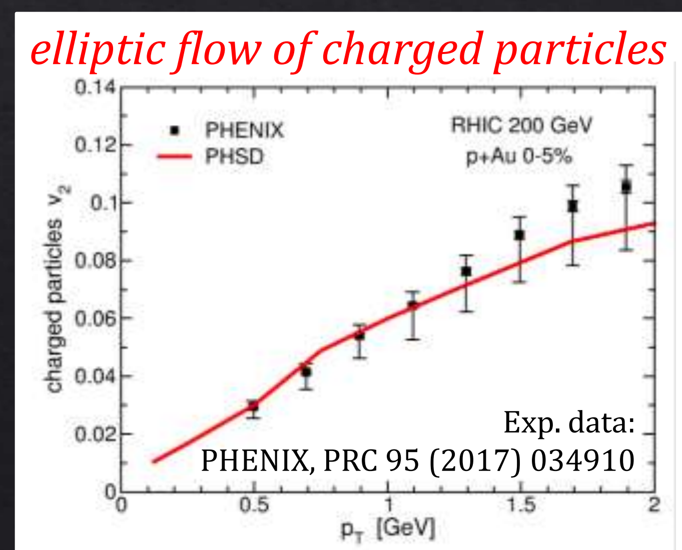

Oliva, Moreau, Voronyuk and Bratkovskaya, Phys. Rev. C 101 (2020) 014917

‚Flavour chemistry' of HIC: K^+/π^+ ‚horn' – 2015

PHSD: even when considering the **creation of a QGP phase**, the **K^+/π^+ ‚horn'** seen experimentally by NA49 and STAR at a bombarding energy ~30 A GeV (FAIR/NICA energies) **remained unexplained (2015)!**

➔ The origin of the 'horn' is not traced back to deconfinement ?!

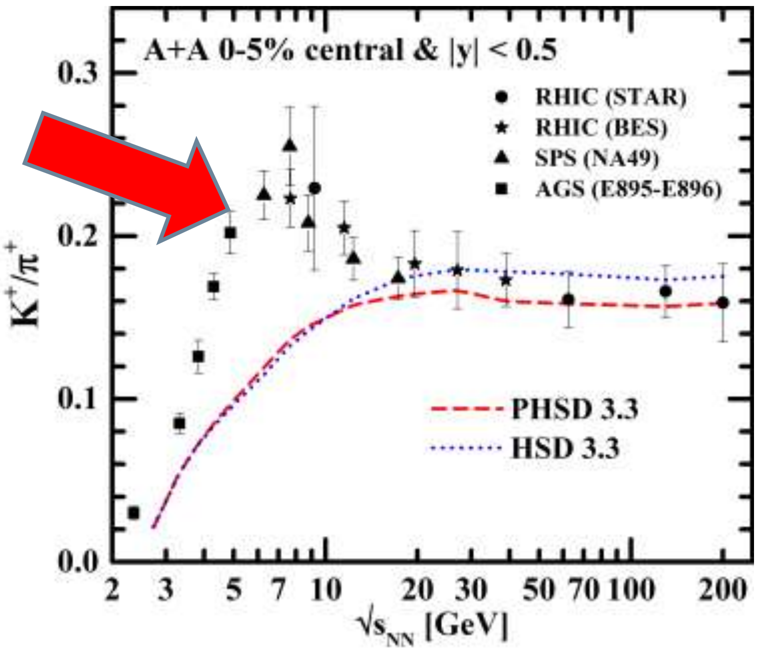

lQCD BMW collaboration:

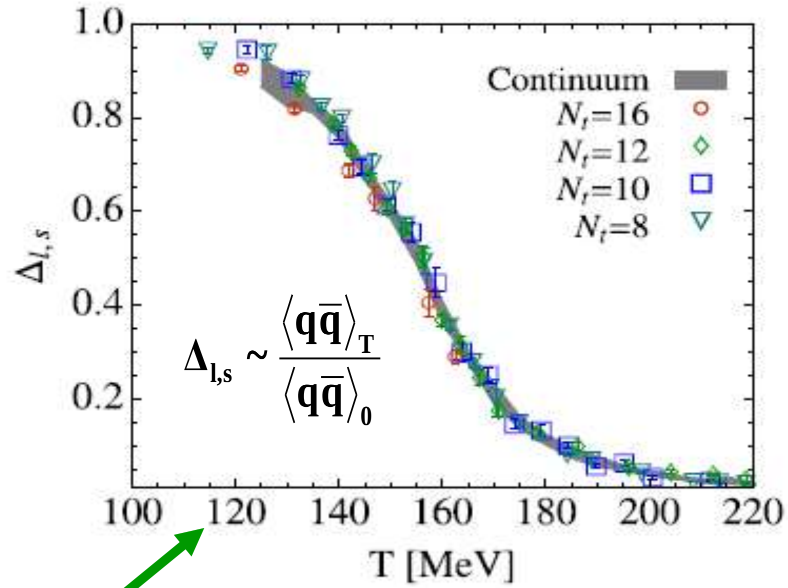

$$\Delta_{l,s} \sim \frac{\langle q\bar{q}\rangle_T}{\langle q\bar{q}\rangle_0}$$

?

Can it be related to chiral symmetry restoration in the hadronic phase?!

W. Cassing, A. Palmese, P. Moreau, E.L. Bratkovskaya, PRC 93, 014902 (2016)

Scalar quark condensate in HIC

PHSD:

Ratio of the scalar quark condensate

$$\frac{<q\bar{q}>}{<q\bar{q}>_V}$$

compared to the vacuum as a function of *x,z (y=0)* at different time *t* for central Au+Au collisions at 30 AGeV

- **restoration of chiral symmetry:** $\langle q\bar{q}\rangle/\langle q\bar{q}\rangle_V \rightarrow 0$

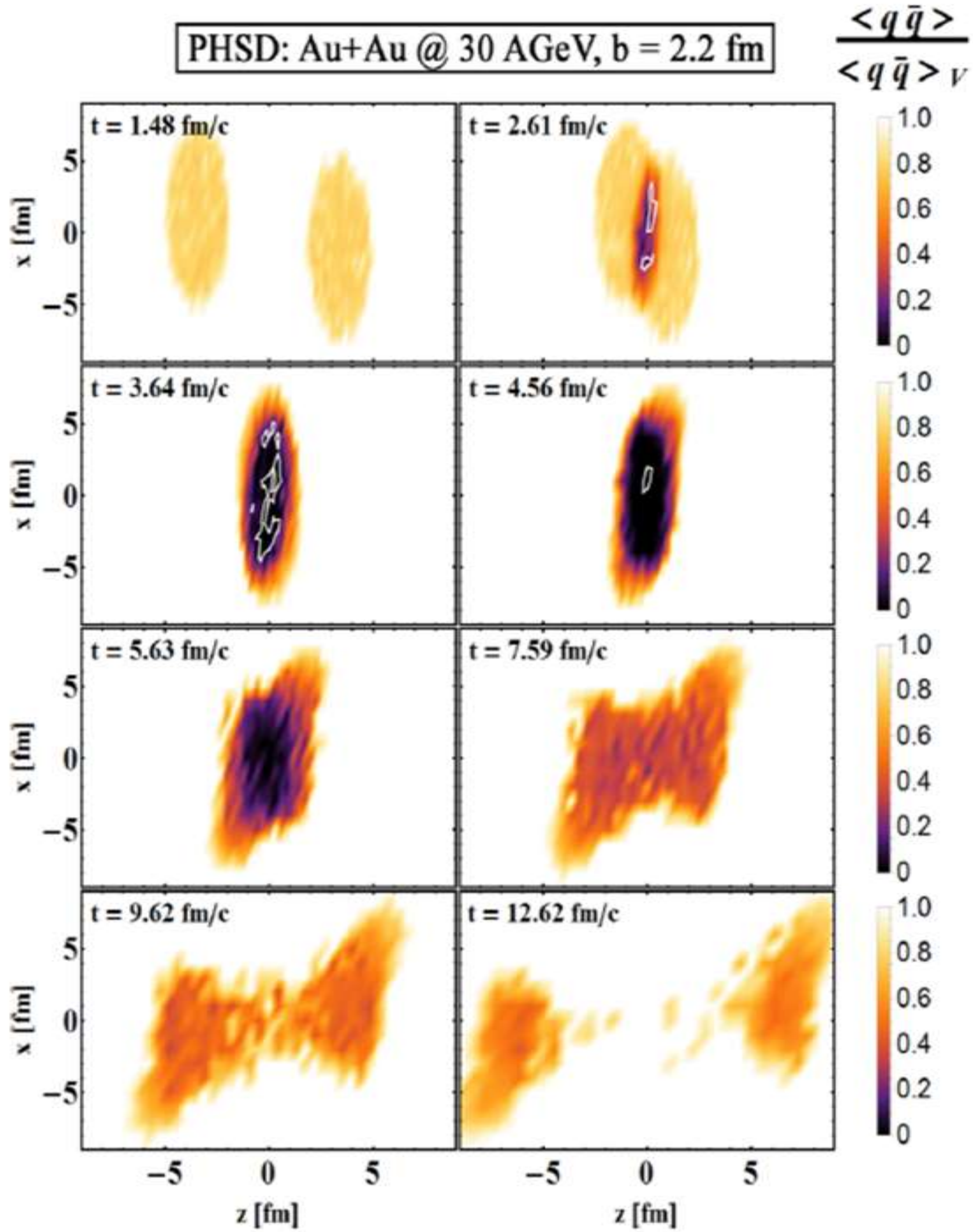

W. Cassing, A. Palmese, P. Moreau, E.L. Bratkovskaya, PRC 93, 014902 (2016), arXiv:1510.04120

Chiral symmetry restoration vs. deconfinement

I. Initial stage of HICs:

Hadronic matter ➔ string formation

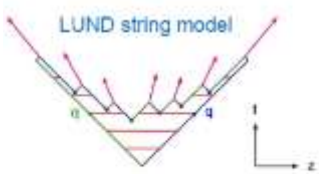

$$\frac{P(s\bar{s})}{P(u\bar{u})} = \frac{P(s\bar{s})}{P(d\bar{d})} = \gamma_S = \exp\left(-\pi \frac{m_S^{*2} - m_q^{*2}}{2\kappa}\right)$$

$$m_q^* = m_q^0 + (m_q^V - m_q^0)\frac{<q\bar{q}>}{<q\bar{q}>_V}$$

II. QGP

(time-like partons, explicit partonic interactions)

III. Hadronic phase

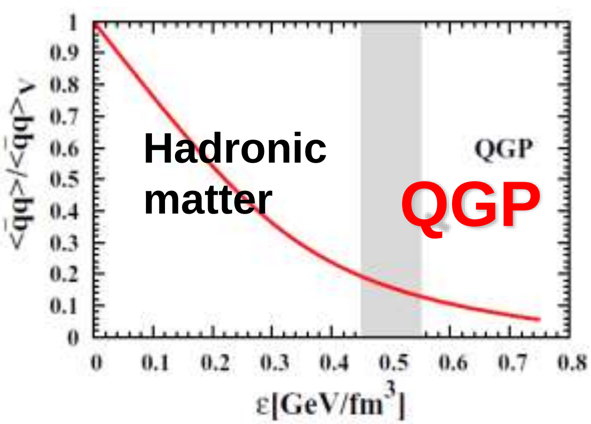

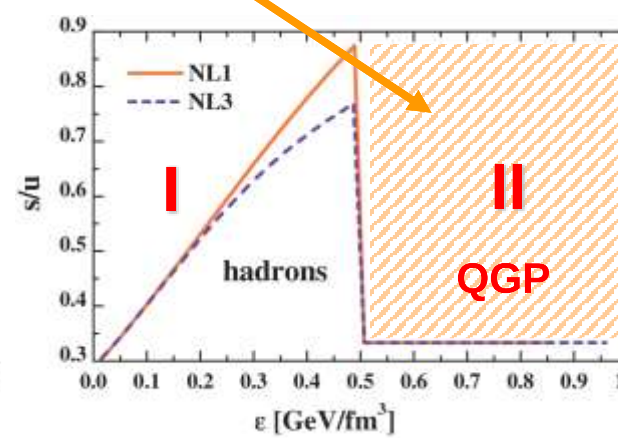

- ❑ **Chiral symmetry restoration via Schwinger mechanism (and non-linear $\sigma - \omega$ model) changes the „flavour chemistry“ in string fragmentation (1PI):**

  $\langle q\bar{q}\rangle/\langle q\bar{q}\rangle_V \rightarrow 0$ ➔ $m_s^* \rightarrow m_s^0$ ➔ **s/u grows**

➔ the strangeness production probability increases with the local energy density ε (up to ε_C) due to the partial chiral symmetry restoration!

Excitation function of hadron ratios and yields

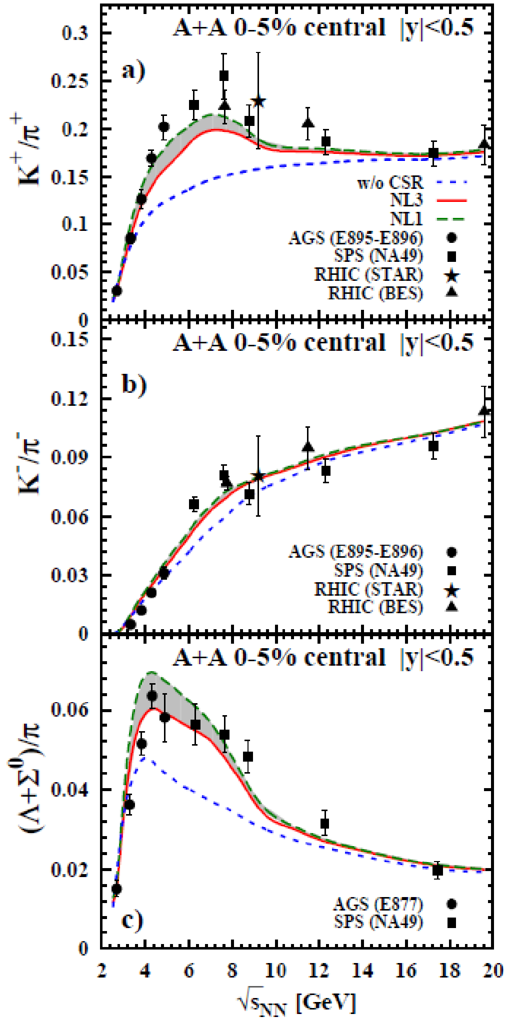

A. Palmese et al., PRC94 (2016) 044912 , arXiv:1607.04073

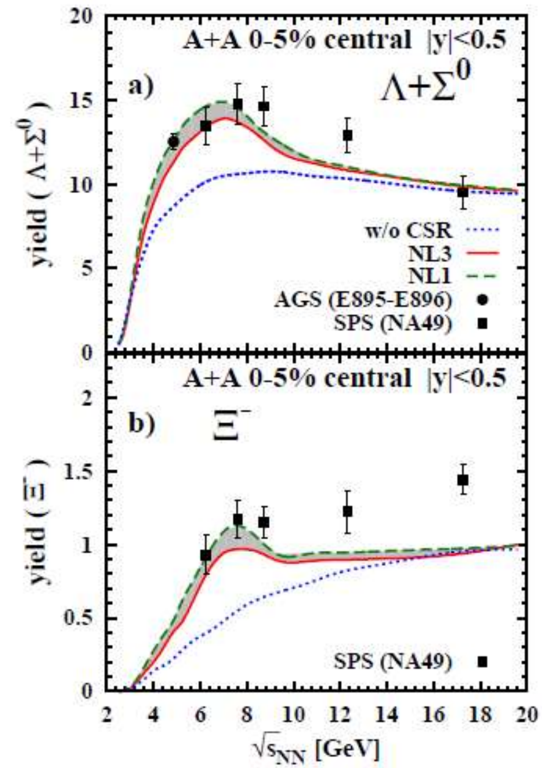

- **Influence of EoS: NL1 vs NL3 ➔ low sensitivity to the nuclear EoS**
- **Excitation function of the hyperons $\Lambda+\Sigma^0$ and Ξ^- show analogous peaks as K^+/π^+, $(\Lambda+\Sigma^0)/\pi$ ratios due to CSR**

Chiral symmetry restoration leads to the enhancement of strangeness production in string fragmentation in the beginning of HICs in the hadronic phase.
➔The „horn“ structure is due to the interplay between CSR and deconfinement (QGP)

Sensitivity to the system size: light A+A collisions

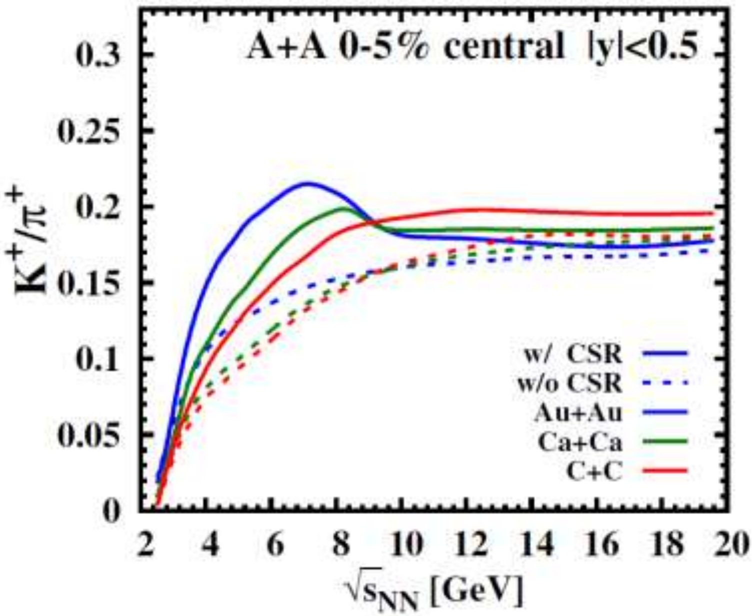

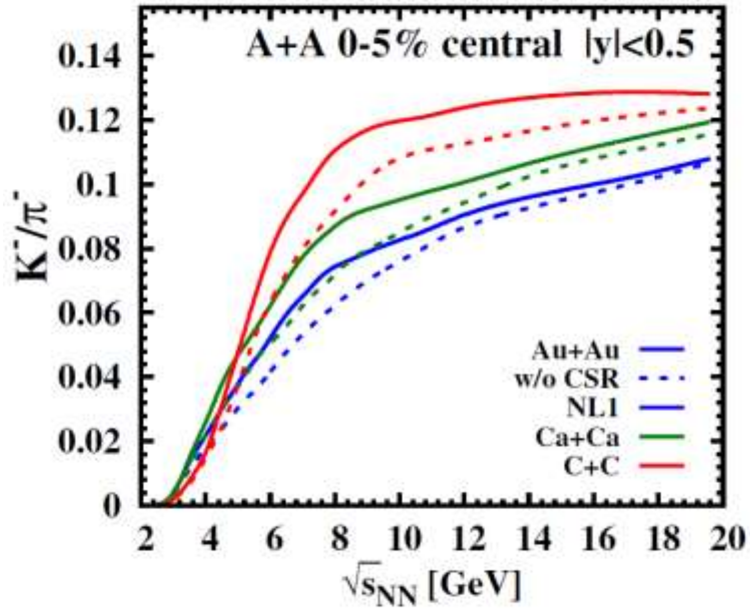

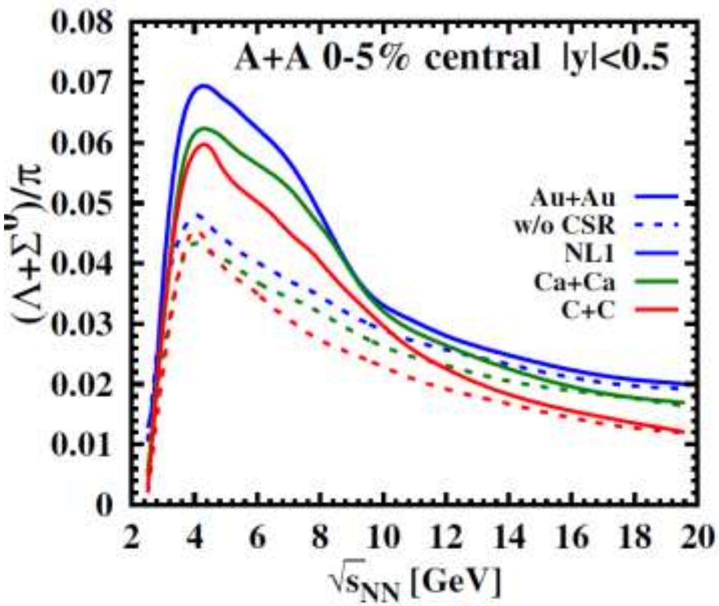

If the system size is smaller:

- **the peak of K^+/π^+ disappears**
- **the peak of $(\Lambda+\Sigma^0)/\pi$ remains in the same position in energy, but getting smaller**

A. Palmese et al., PRC94 (2016) 044912 , arXiv:1607.04073

Sensitivity to the system size: p+A collisions

- In p+A collisions strange to non-strange particle ratios show no peaks

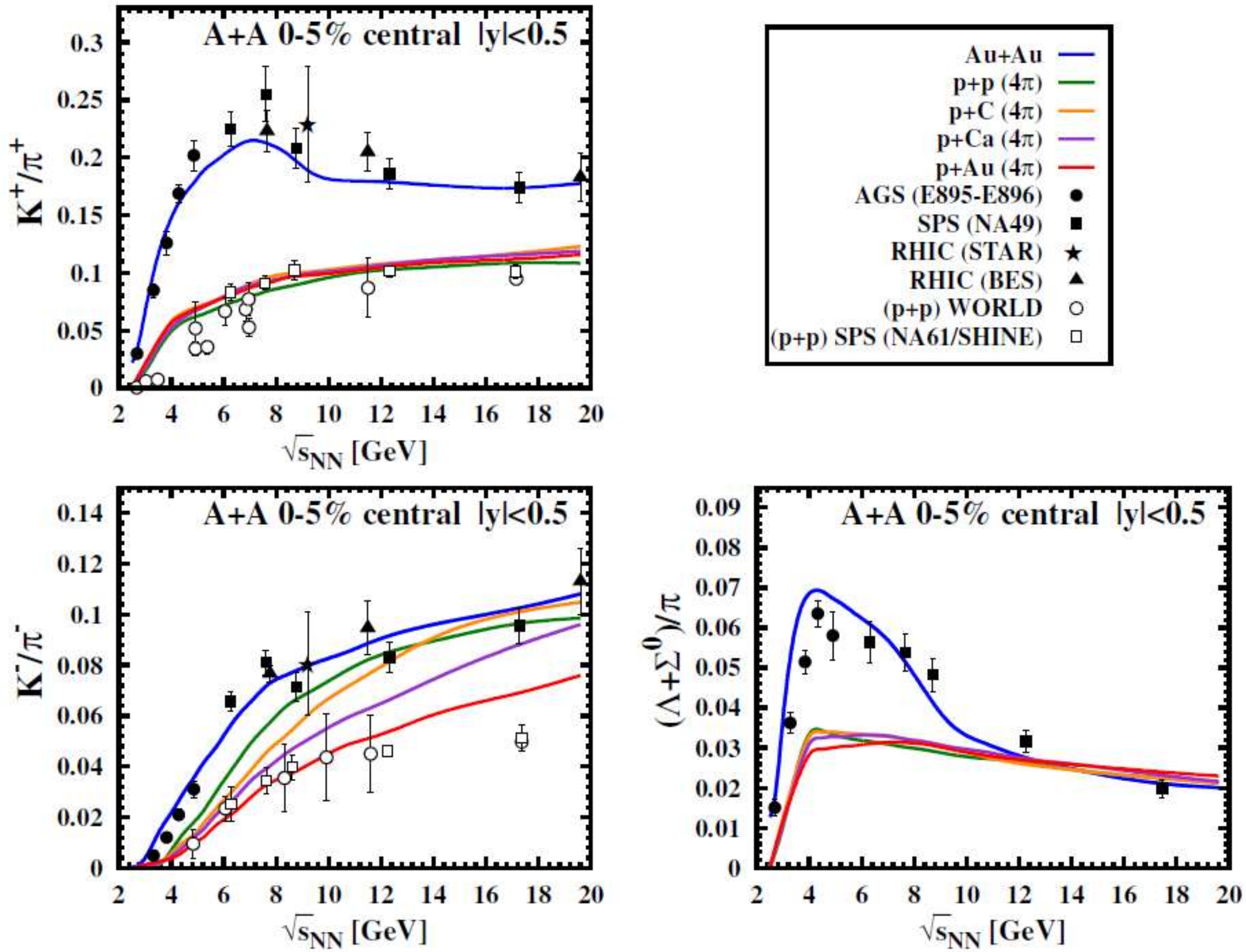

A. Palmese et al., PRC94 (2016) 044912 , arXiv:1607.04073

Cluster and hypernuclei formation within PHQMD

J. Aichelin, E. Bratkovskaya, A. Le Fevre, V. Kireyeu, V. Kolesnikov,
Y. Leifels, V. Voronyuk, G. Coci,
Phys. Rev. C 101, 044905 (2020), arXiv:1907.03860

Clusters and hypernuclei production in HICs

- Clusters are very abundant at low energy

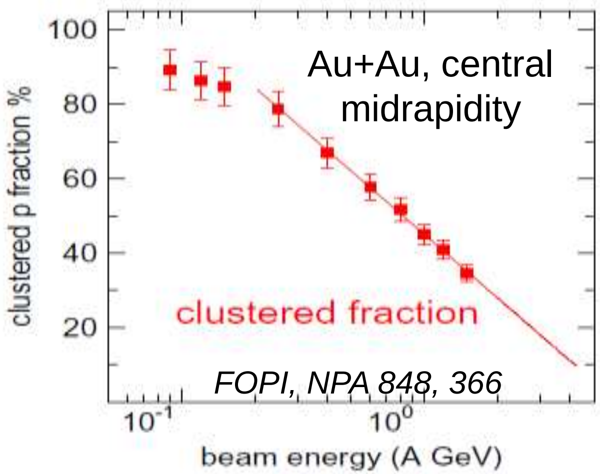

- to explore new physics opportunities like
- hyper-nucleus formation
- possible signals of the 1st order phase transition
- origin of cluster formation at midrapidity (RHIC, LHC):

Experimental observables:

...

Clusters and (anti-) hypernuclei

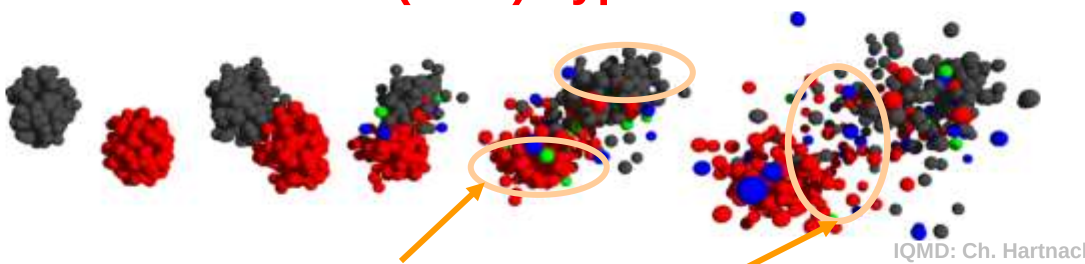

- projectile/target spectators➔ heavy cluster formation
- midrapidity➔ light clusters

! Hyperons are created in participant zone

(Anti-) hypernuclei production:

- at mid-rapidity by Λ coalessance during expansion
- at projectile/target rapidity by rescattering/absorption of Λ by spectators

High energy HIC: ‚Ice in a fire' puzzle: how the weakly bound objects can be formed in a hot enviroment ?!

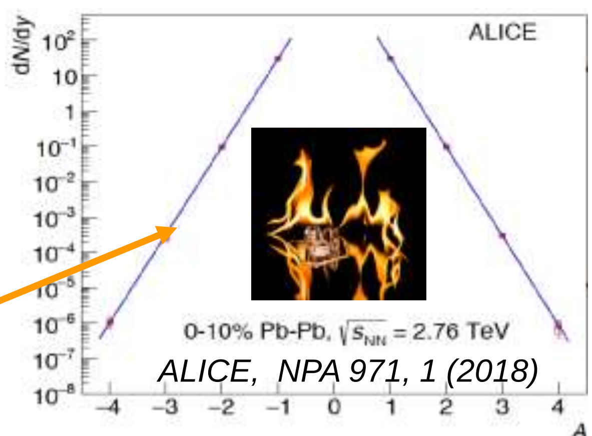

PHQMD

The goal: to develop a **unified n-body microscopic transport approach** for the description of heavy-ion dynamics and dynamical cluster formation from low to ultra-relativistic energies

Realization: combined model **PHQMD = (PHSD & QMD) & SACA**

Parton-Hadron-Quantum-Molecular Dynamics

↓

Initialization → propagation of baryons:
QMD (Quantum-Molecular Dynamics)

↓

Propagation of partons (quarks, gluons) and mesons
+ collision integral = interactions of hadrons and partons (QGP)
from PHSD (Parton-Hadron-String Dynamics)

↓

Clusters recognition:
SACA (Simulated Annealing Clusterization Algorithm)
vs. MST (Minimum Spanning Tree)

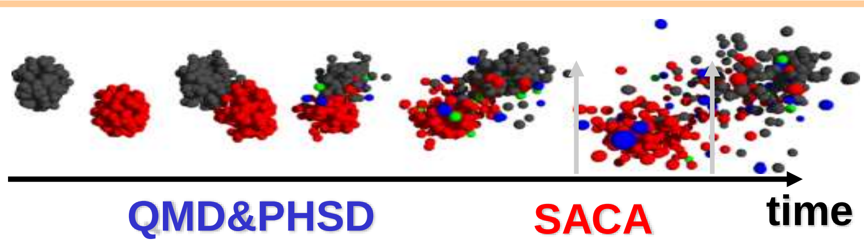

Cluster recognition: Minimum Spanning Tree (MST)

The Minimum Spanning Tree (MST) is a cluster recognition method applicable for the (asymptotic) final states where coordinate space correlations may only survive for bound states.

The MST algorithm searches for accumulations of particles in coordinate space:

1. Two particles are 'bound' if their distance in coordinate space fulfills

$$\left|\vec{r}_i - \vec{r}_j\right| \leq 2.5\, fm$$

2. Particle is bound to a cluster if it bounds with at least one particle of the cluster.

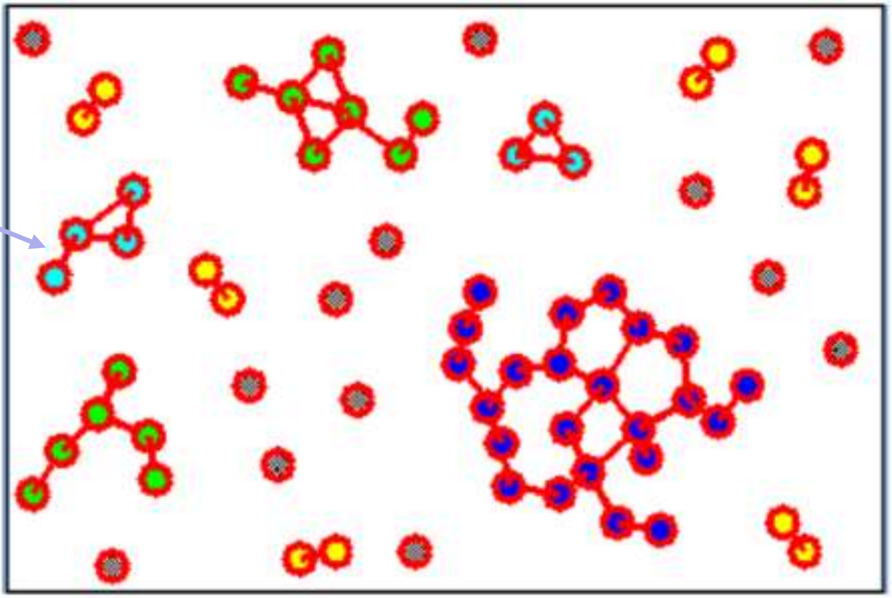

* Remark:
inclusion of an additional momentum cuts (coalescence) lead to a small changes: particles with large relative momentum are mostly not at the same position

R. K. Puri, J. Aichelin, J.Comp. Phys. 162 (2000) 245-266

Simulated Annealing Clusterization Algorithm (SACA)

Basic ideas of clusters recognition by SACA:

Based on idea by Dorso and Randrup (Phys.Lett. B301 (1993) 328)

- **Take the positions and momenta of all nucleons at time t**
- **Combine them in all possible ways into all kinds of clusters or leave them as single nucleons**
- **Neglect the interaction among clusters**
- **Choose that configuration which has the highest binding energy:**

Take randomly 1 nucleon out of a cluster

Add it randomly to another cluster

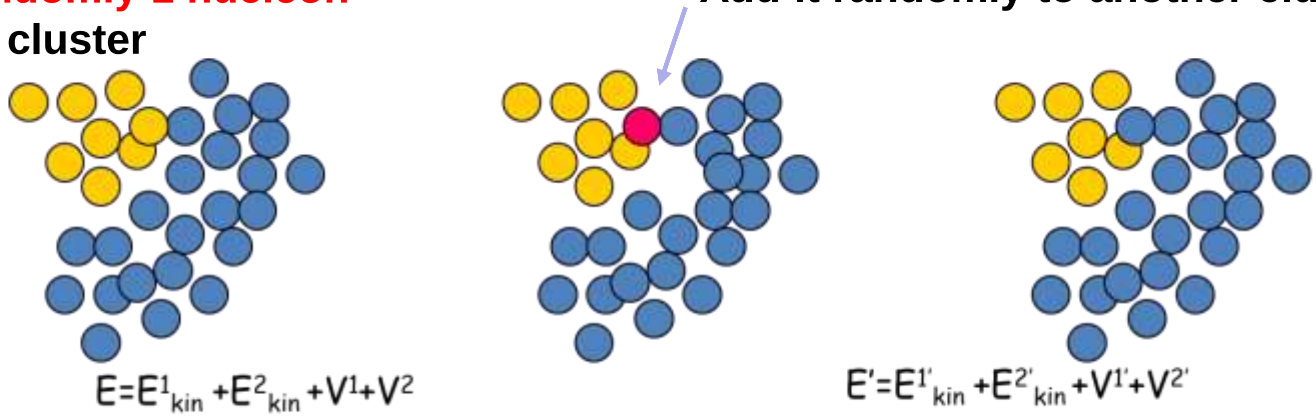

If E' < E take a new configuration
If E' > E take the old configuration with a probability depending on E'-E
Repeat this procedure many times

→ **Leads automatically to finding of the most bound configurations**

R. K. Puri, J. Aichelin, PLB301 (1993) 328, J.Comput.Phys. 162 (2000) 245-266;
P.B. Gossiaux, R. Puri, Ch. Hartnack, J. Aichelin, Nuclear Physics A 619 (1997) 379-390

PHQMD: light clusters at AGS energies

The invariant multiplicities for p, d, t, ^{3}He, ^{4}He at p_T <0.1 GeV versus rapidity

Au+Au, 11 AGeV, 10% central

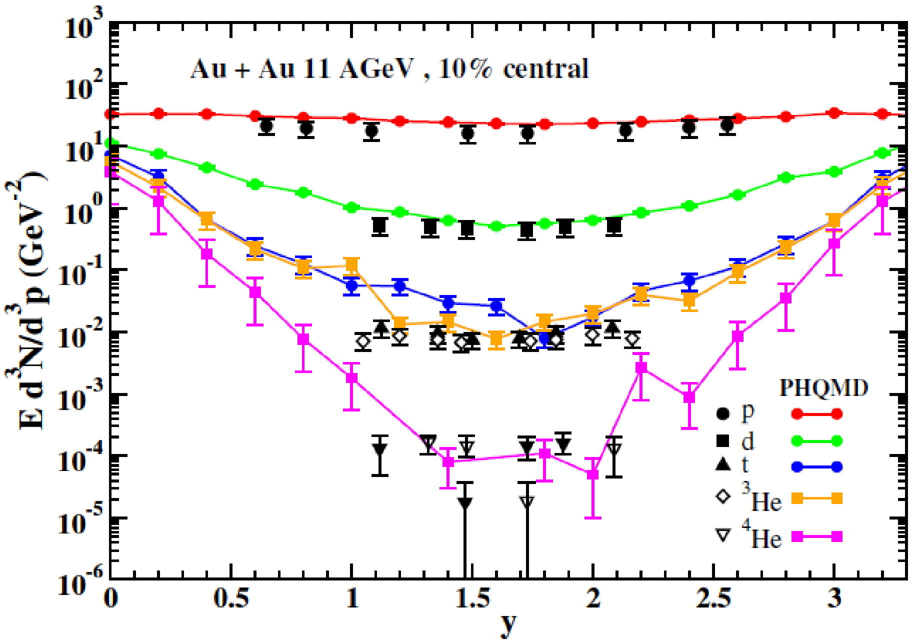

Au+Au, 11 AGeV, minimal bias

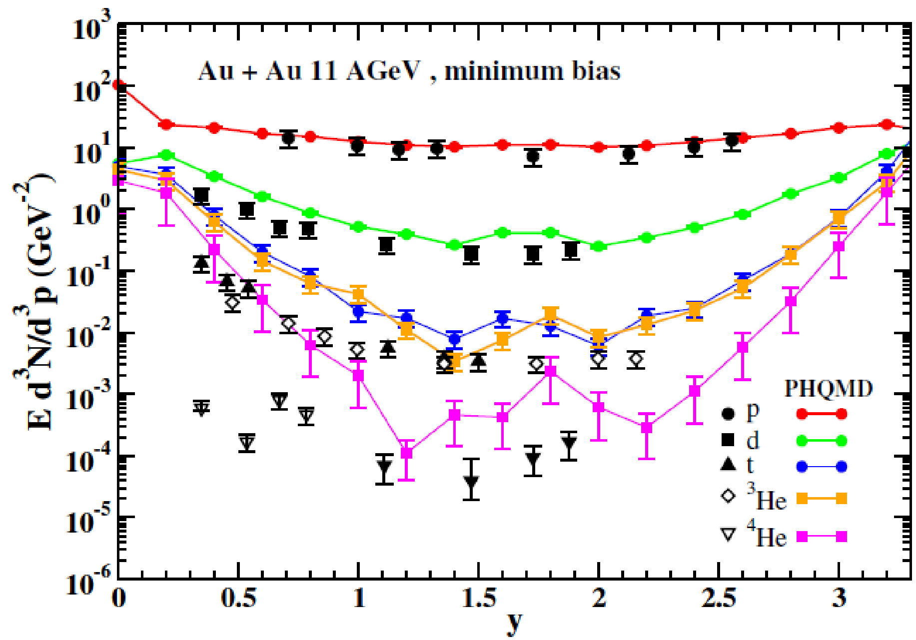

PHQMD: cluster recognition by MST provides a reasonable description of exp. data on light clusters at AGS energies

PHQMD: hypernuclei

PHQMD results (with a hard EoS and MST algorithm) for the rapidity distributions of all charges, Z = 1 particles, Z=2, Z>2, as well as Λ's, hypernuclei A≤4 and A>4 for Au+Au at 4 and 10AGeV

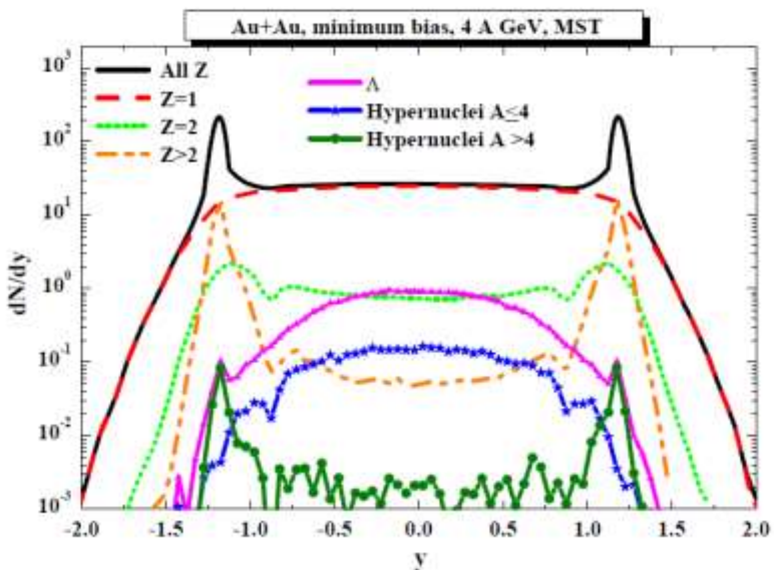

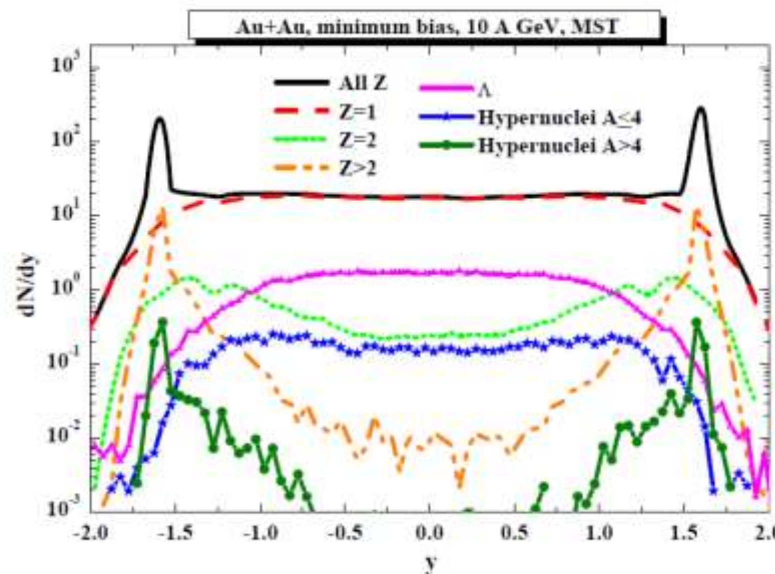

The multiplicity of light hypercluster vs. impact parameter b for Au+Au, 4 AGeV

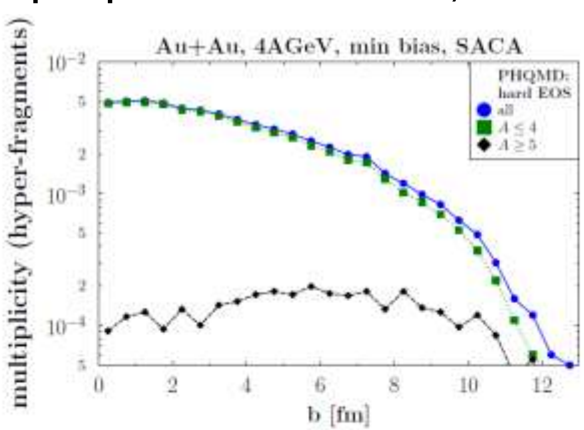

- **Central collisions → light hypernuclei**
- **Peripheral collisions → heavy hypernuclei**

Penetration of Λ's, produced at midrapidity, to target/projectile region due to rescattering

→ Possibility to study ΛN interaction

PHQMD: collectivity of clusters

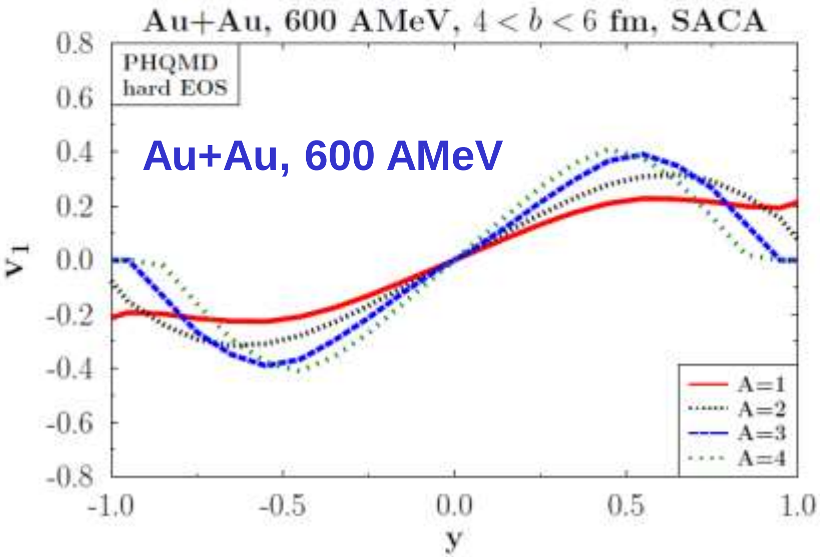

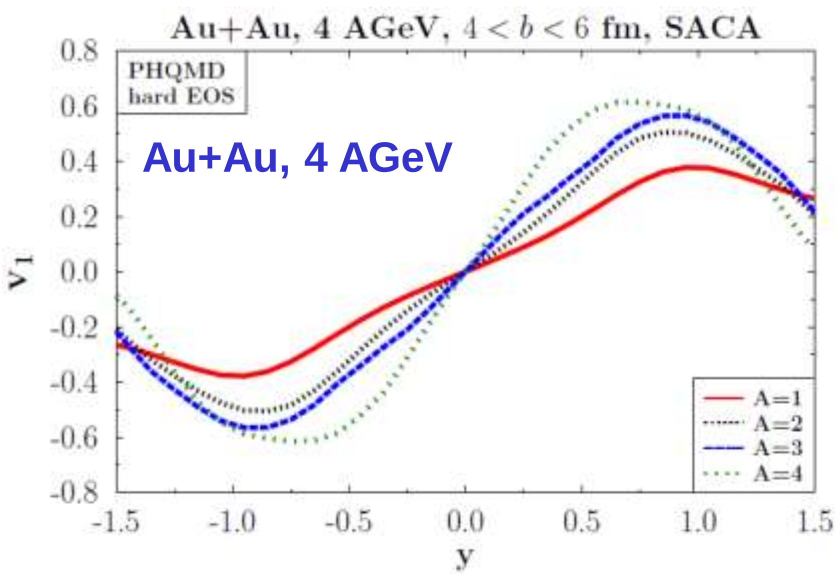

PHQMD with hard EoS, with SACA:
v_1 of light clusters (A=1,2,3,4) vs rapidity
for mid-central Au+Au at 600 AMeV, 4AGeV

- **v_1 : quite different for nucleons and clusters (as seen in experiments)**
- **Nucleons come from participant regions (→ small density gradient) while clusters from interface spectator-participant (strong density gradient)**
- **v_1 increases with E_{beam}**
  → larger density gradient

Vorticity, polarization phenomena in relativistic heavy-ion collisions

Vorticity and Λ polarization in HICs

PHENIX: Nature 548, 62 (2017), arXiv:1701.06657
"Global hyperon polarization in nuclear collisions: evidence for the most vortical fluid"

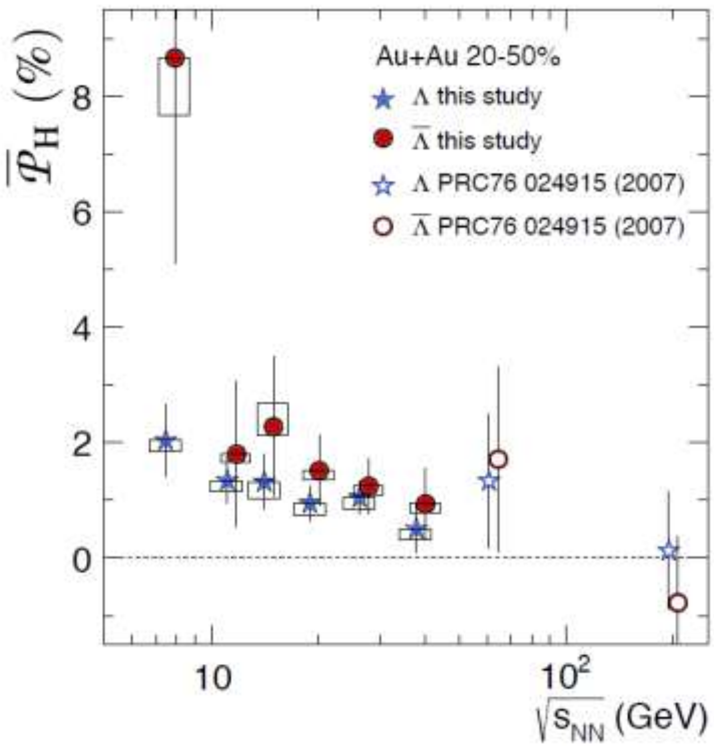

Λ **polarization can be measured by angular distribution of the protons in the decay Λ→p+π⁻**

$$\frac{dN}{d\Omega^*} = \frac{1}{4\pi}\left(1 + \alpha_\Lambda \mathbf{P}_\Lambda^* \cdot \hat{\mathbf{p}}^*\right)$$

The fluid vorticity may be estimated from the data using the hydrodynamic relation:

F. Becattini et al., PRC95 (2017) 054902

$$\omega = k_B T \left(\overline{\mathcal{P}}_{\Lambda'} + \overline{\mathcal{P}}_{\overline{\Lambda}'}\right)/\hbar.$$

PHENIX: averaged fluid vorticity in HIC:

$$\omega \approx (9 \pm 1) \times 10^{21}\ \mathrm{s}^{-1}$$

This by far surpasses the vorticity of all other known fluids:

- **solar subsurface flow: $10^{-7}s^{-1}$**
- **supercell tornado cores: $10^{-1}s^{-1}$**
- **rotating, heated soap bubbles: 10^{2} s^{-1}**
- **superfluid nanodroplets: $10^{7}s^{-1}$**

➔ Hot and dense matter created in the HICs is the most vortical fluid !

Vorticity & Λ polarization in HIC

F. Becattini et al., PRC95 (2017) 054902
Eur. Phys. J C75 (2015) 406

Relativistic kinematic vorticity

$$\omega_{\mu\nu} = \frac{1}{2}(\partial_\nu u_\mu - \partial_\mu u_\nu) \qquad u_\nu(t,\vec{x}) = \gamma(1, \vec{v}(t,\vec{x}))$$

Relativistic thermal vorticity

$$\varpi_{\mu\nu} = \frac{1}{2}(\partial_\nu \beta_\mu - \partial_\mu \beta_\nu) \qquad \beta_\nu = \frac{u_\nu}{T}$$

← Thermodynamic equilibrium

Polarization due to spin-orbital interaction → Spin vector:

$$S^\mu(x,p) = -\frac{s(s+1)}{6m}(1 \pm n(x,p))\varepsilon^{\mu\nu\lambda\delta}\, \varpi_{\nu\lambda}\, p_\delta$$

***n(x,p)* – Bose/Fermi distribution**

Polarization of Λ: $P = 2\frac{\mathbf{S}^* \cdot \mathbf{L}}{|L|}$

S* - spin vector in the rest frame of Λ,
L- angular momentum of the system

Additional complication: sizable feed-down of Λ from resonance decays:

$$\Sigma^0 \to \Lambda + \gamma,\ \Sigma^* \to \Lambda + \pi,\ \Xi \to \Lambda + \pi$$

$$\Sigma^* \to \Sigma + \pi \to \Lambda + \pi + \gamma,\ \Xi^* \to \Xi + \pi \to \Lambda + \pi + \pi$$

In decays, the Λ inherit a fraction of polarization from the initial (parent) states

PHSD: Vorticity & Λ polarization in HIC

Study of vorticity and polarization of Λ within the PHSD:

E.E. Kolomeitsev, V.D. Toneev, V. Voronyuk, PRC 97 (2018) 064902

- **Influence of chiral symmetry restoration effects in (anti-) hyperon production**

Au+Au, $s^{1/2}$=7.7 GeV, b=7.5 fm

Hyperons→

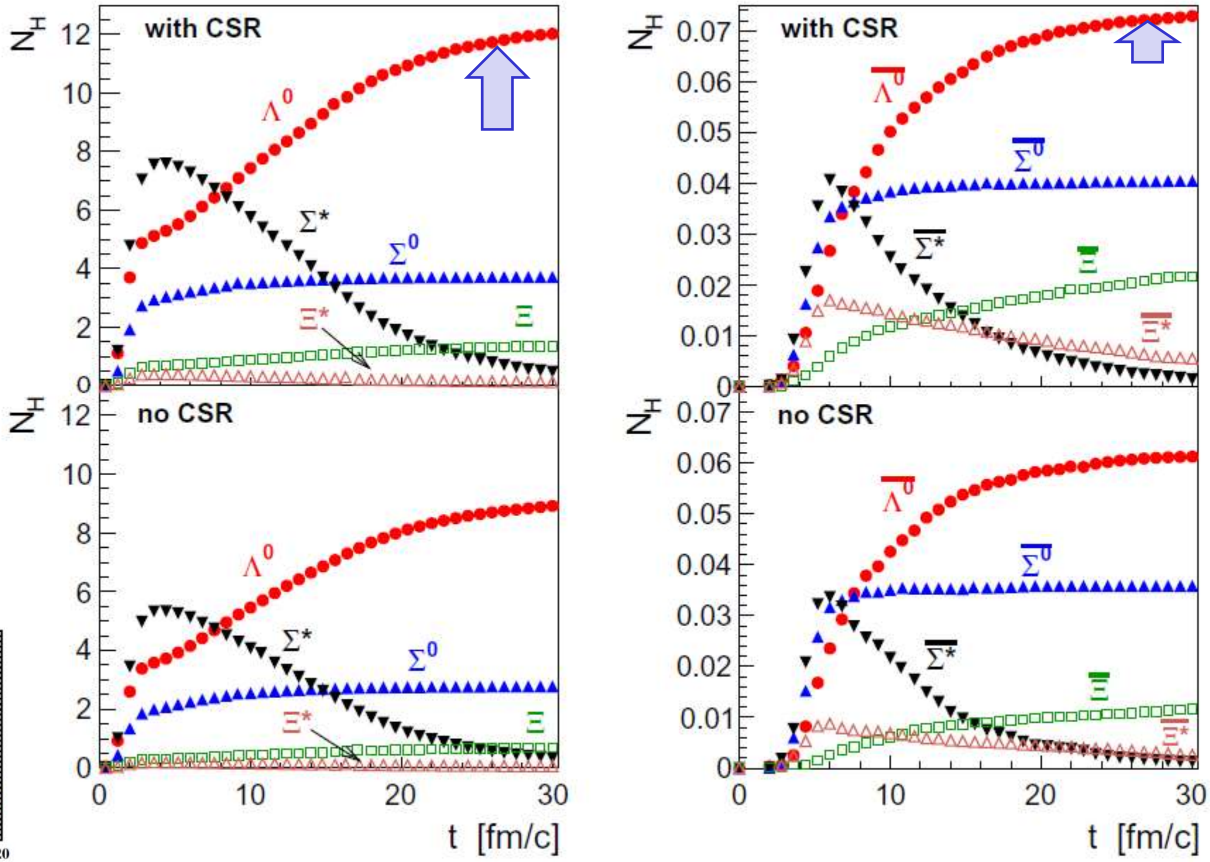

← Antihyperons

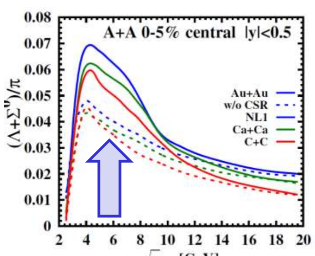

PHSD: Vorticity & Λ polarization in HICs

E.E. Kolomeitsev, V.D. Toneev, V. Voronyuk, PRC 97 (2018) 064902

Au+Au, $s^{1/2}$=7.7 GeV, b=7.5 fm

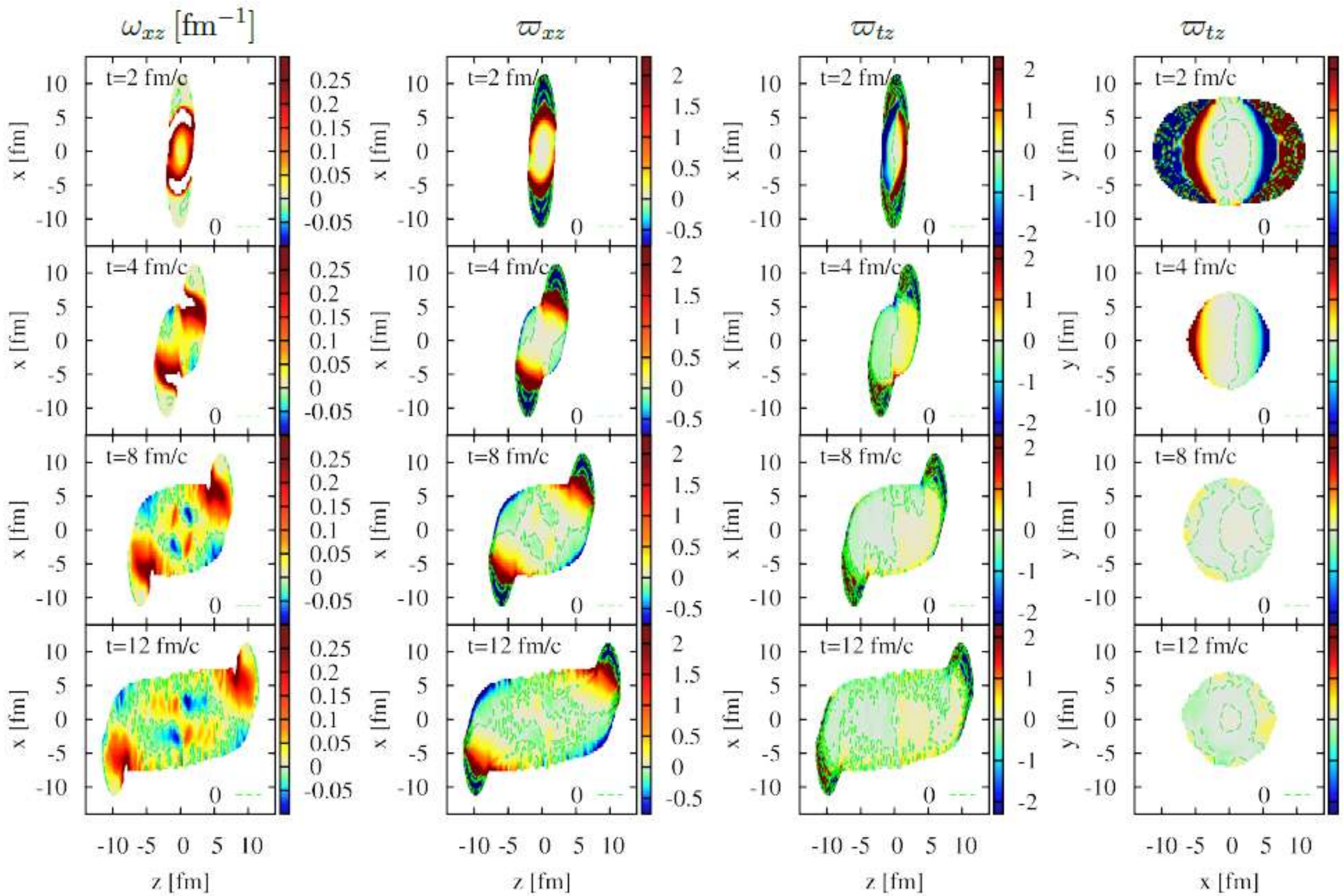

The vorticity is larger at the border between participant and spectator matter

PHSD: Vorticity & Λ polarization in HICs

E.E. Kolomeitsev, V.D. Toneev, V. Voronyuk, PRC 97 (2018) 064902

Thermal vorticity distribution of Λ and Σ* hyperons (upper row) and anti-Λ and anti-Σ* (lower row) at different times

Au+Au, $s^{1/2}$=7.7 GeV, b=7.5 fm

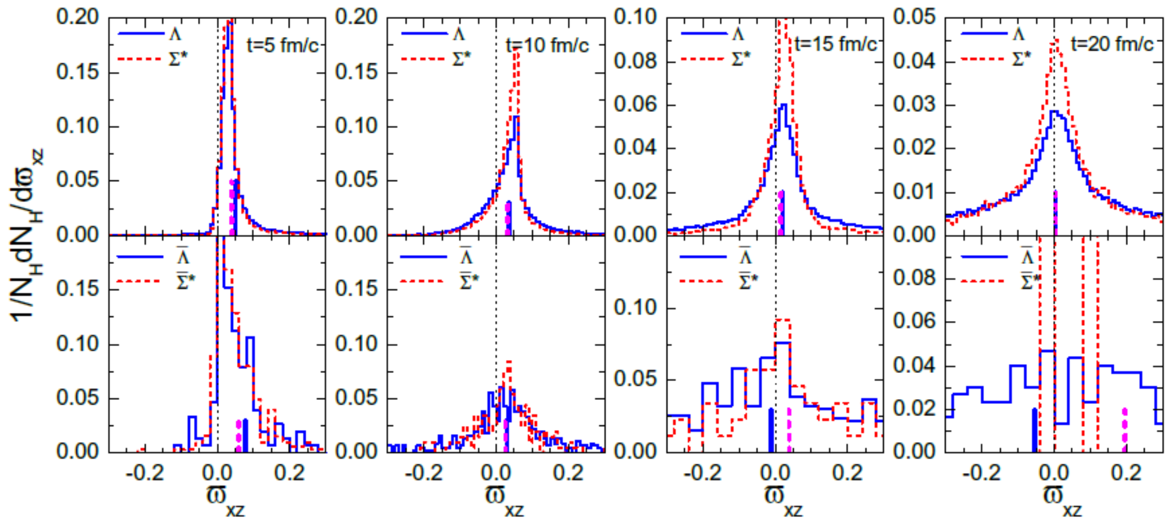

Vertical lines- averaged values of the thermal vorticity
→ decreases with time
(other components are symmetric)

$$S_y \sim \varpi_{xz}$$

Λ polarization vs pseudorapidity

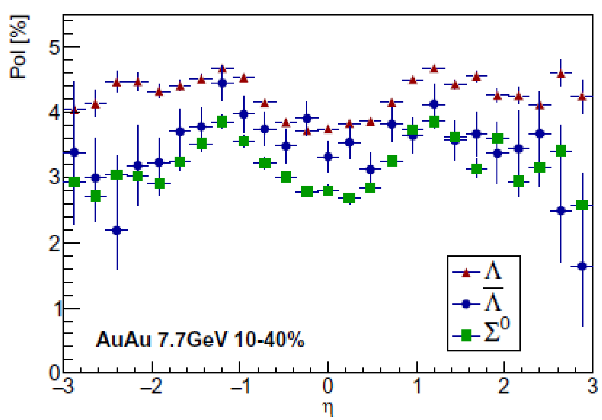

Λ polarization vs centrality

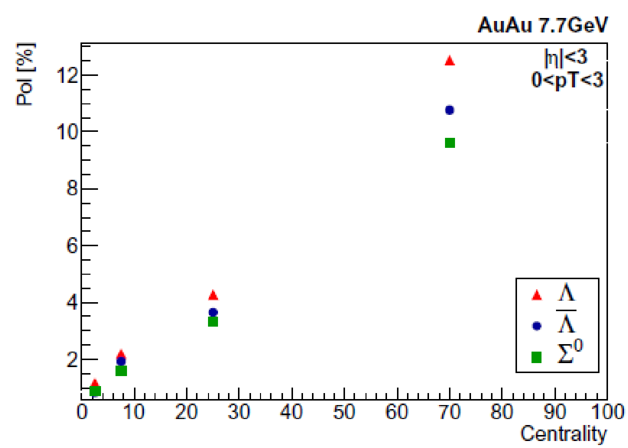

PHSD: Vorticity & Λ polarization in HICs

E.E. Kolomeitsev, V.D. Toneev, V. Voronyuk, PRC 97 (2018) 064902

Au+Au, $s^{1/2}$=7.7 GeV, b=7.5 fm

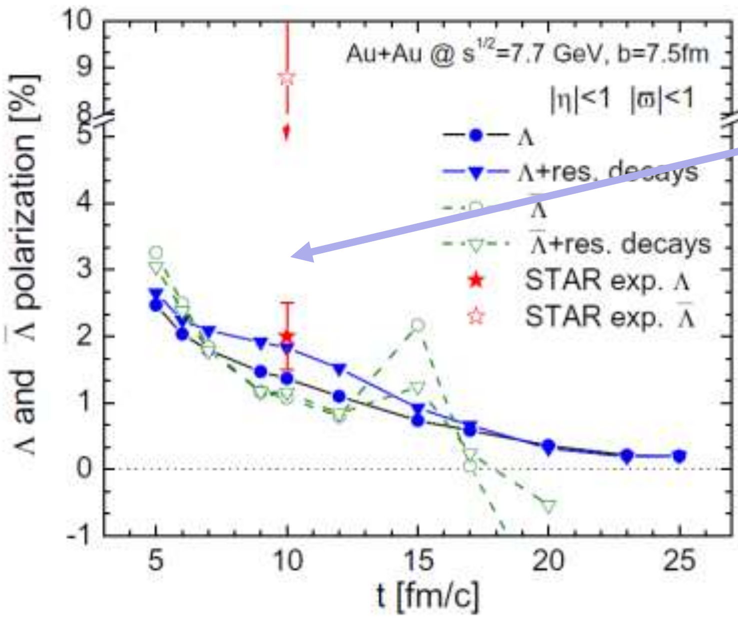

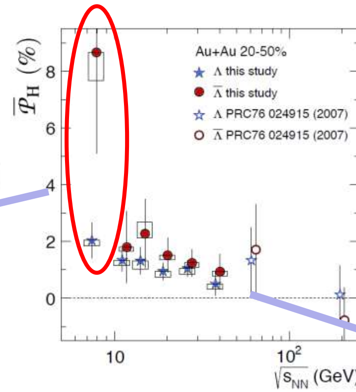

Excitation function P_H

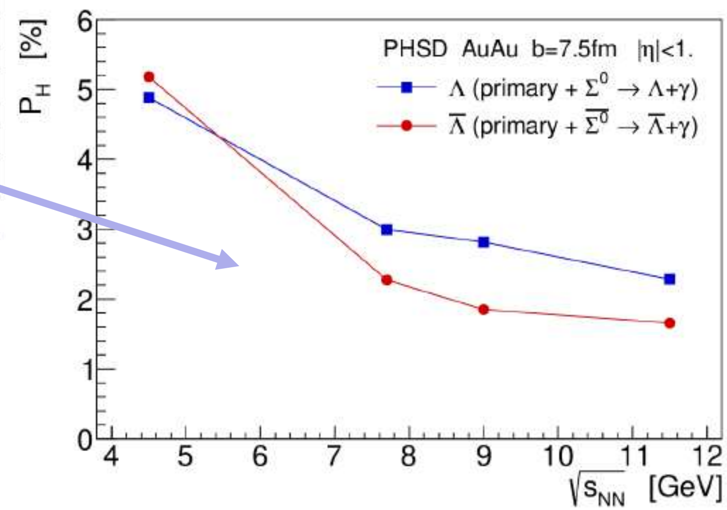

➔ **PHSD explains Λ polarization very well!**

- **Why the polarization for production of the anti-Λ hyperons is higher than for Λ at Au+Au, $s^{1/2}$=7.7 GeV?**
- **Possible influence of magnetic fields?!**

➔ **NICA (SPD) measurements are very needed!**

Parity-odd effects - vorticity and helicity

Helicity:

O. Teryaev and R.Usibov, PRC92 (2015) 014906

$$H_{\uparrow} = \int (\vec{v}, rot\vec{v}) dV, v_y > 0 \qquad H_{\downarrow} = \int (\vec{v}, rot\vec{v}) dV, v_y < 0$$

HSD: Au+Au, $s^{1/2}$=5 GeV, b=4 fm

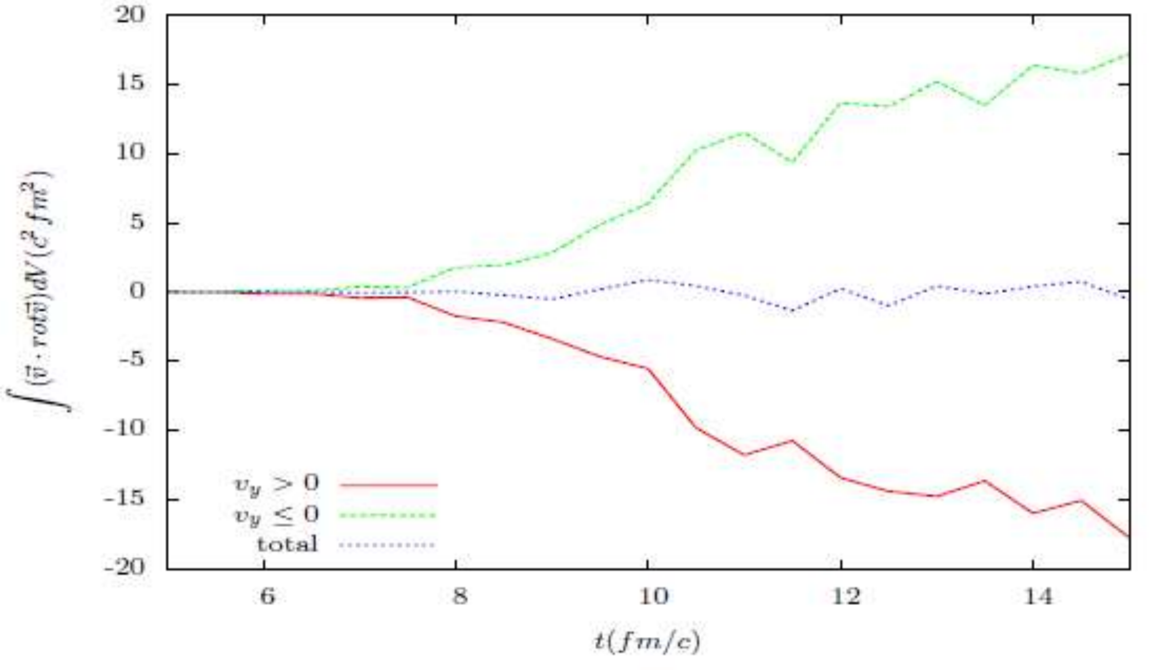

Handedness:

$$H_{||} = \frac{N_l - N_r}{N_l + N_r}$$

➔ **Helicity, Handedness - interesting opportunities for the SPD!**

Polarization of ϕ-mesons in HIC

Xin-Li Sheng, Lucia Oliva, Qun Wang, PRD 101 (2020) 096005

Angular distribution of ϕ decay: $\frac{dN}{d\cos\theta} = \frac{3}{4}\left[(1-\rho_{00}) + (3\rho_{00}-1)\cos^2\theta\right]$

Spin density matrix ρ_{00} measures a spin alignment of ϕ mesons: if $\rho_{00} \neq 1/3$, the distribution is anisotropic and the spin of ϕ meson is aligned to the spin quantization direction

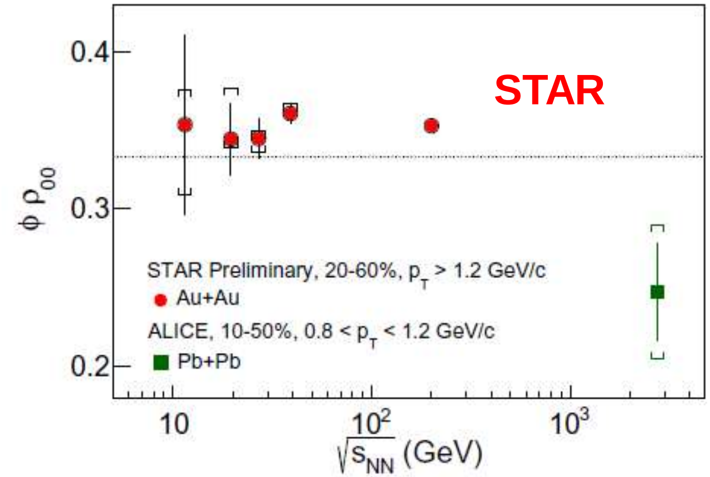

Experiment: STAR $\rho^{\phi}_{00} > 1/3$ **(for K* ρ_{00} <1/3)**

Theoretical expectation:

$$\rho^{\phi}_{00} \approx \underbrace{\frac{1}{3} - \frac{4}{9}\left\langle P^y_{\Lambda} P^y_{\bar{\Lambda}}\right\rangle}_{c_\Lambda} - \underbrace{\frac{1}{27m_s^2}\left\langle \mathbf{p}^2\right\rangle_\phi \left\langle \varepsilon_z^2 + \varepsilon_x^2\right\rangle}_{c_\varepsilon \text{ (vorticity)}} + \underbrace{\frac{e^2}{243 m_s^4 T_{\text{eff}}^2}\left\langle \mathbf{p}^2\right\rangle_\phi \left\langle E_z^2 + E_x^2\right\rangle}_{c_E \sim 10^{-5} \text{ (EMF from PHSD)}} \quad < 1/3$$

$$\rho^{\phi}_{00} \approx \frac{1}{3} + c_\Lambda + c_\varepsilon + c_E + c_\phi \quad > 1/3$$

New term c_ϕ: the contribution from the polarization of the s/sbar quarks via the spin-orbit interaction in the ϕ field

$$\phi^\mu \approx -(g_\phi/m_\phi^2) J_s^\mu \qquad J_s^\mu(t,\mathbf{x}) = (\rho_s, \mathbf{J}_s) = (\rho_s, j_s^x, j_s^y, j_s^z),$$

$$c_\phi \equiv \frac{g_\phi^4}{27 m_s^4 m_\phi^4 T_{\text{eff}}^2}\left\langle \mathbf{p}^2\right\rangle_\phi \left\langle \tilde{E}^2_{\phi,z} + \tilde{E}^2_{\phi,x}\right\rangle$$

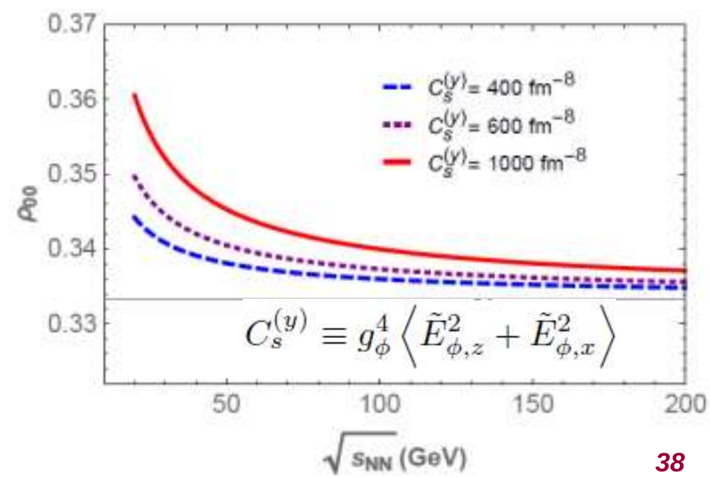

Electromagnetic probes of the QGP and in-medium effects: dileptons and thermal photons

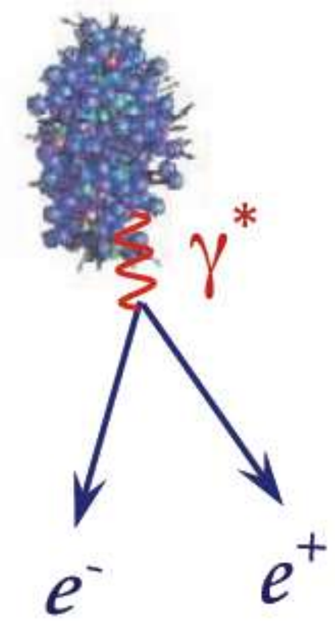

Dilepton sources

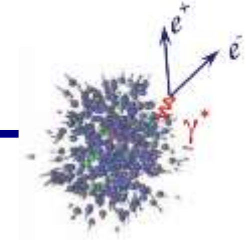

- **from the QGP via partonic (q,qbar, g) interactions:**

PHSD: non-perturbative QGP → DQPM

- **from hadronic sources:**

in-medium effects

Plot from A. Drees

- **direct decay of vector mesons (ρ,ω,φ,J/Ψ,Ψ')**

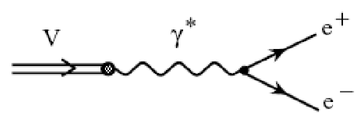

- **Dalitz decay of mesons and baryons (π^0,η, Δ,…)**

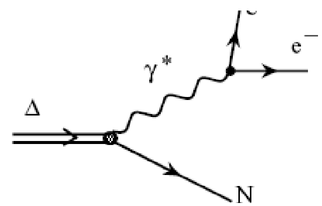

- **correlated D+Dbar pairs**

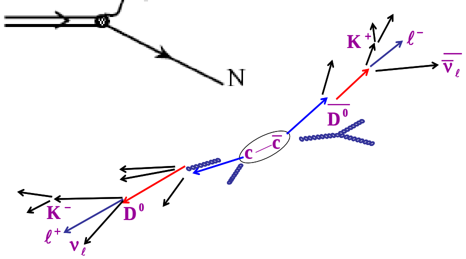

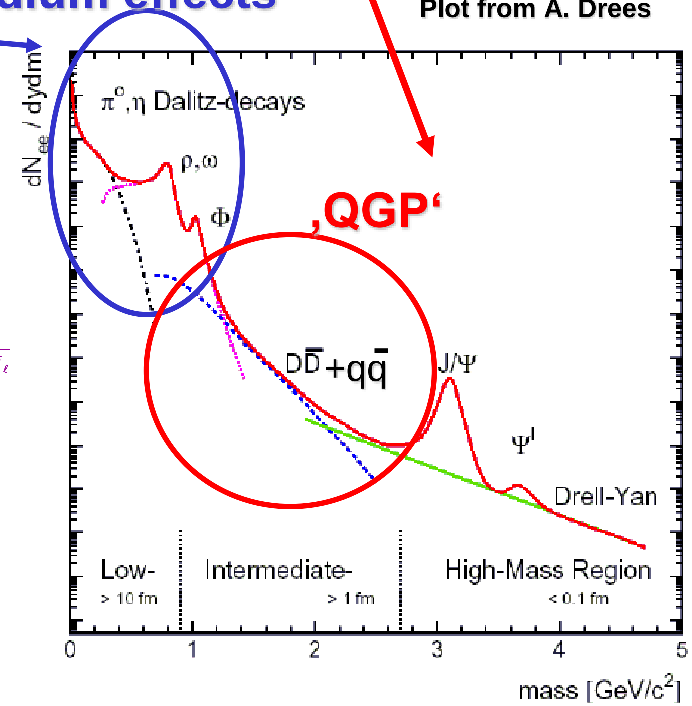

- **radiation from multi-meson reactions ($\pi+\pi$, $\pi+\rho$, $\pi+\omega$, $\rho+\rho$, $\pi+a_1$) - '4π'**

What is the best energy range to observe dileptons from QGP?

A decade of search for the solution of the DLS puzzle

Reminder of the history

✓ Constraints on π, η by TAPS data:
HSD: good description of TAPS data on π, η multiplicities and m_T-spectra
=> π (Δ), η dynamics under control !

Other channels: ρ, ω:
- accounting for in-medium effects (collisional broadening of vector meson spectral functions, dropping vector meson masses) does not provide enough enhancement at intermediate M
- contribution from N(1520)

[E.B.&C.M. Ko, PLB 445 (1999) 265]

and higher baryonic resonances are small

[Gy. Wolf et al., PRC67 (2003) 044002]

Also:
- accounting for anisotropies in e+e- emission gives only a small effect

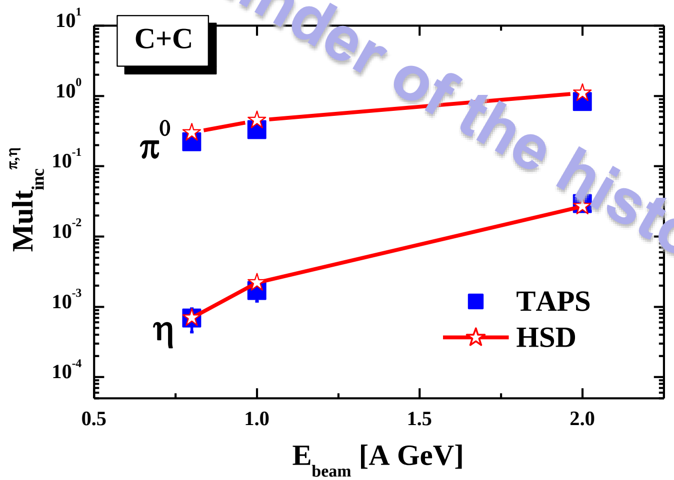

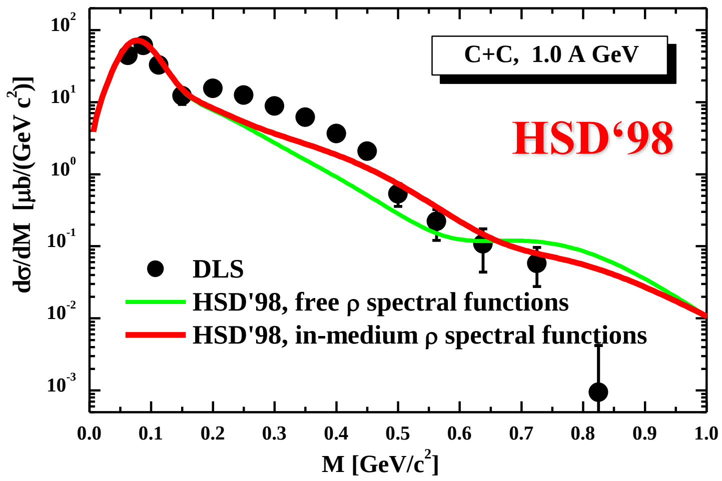

Bremsstrahlung – a new view on an ‚old‘ story

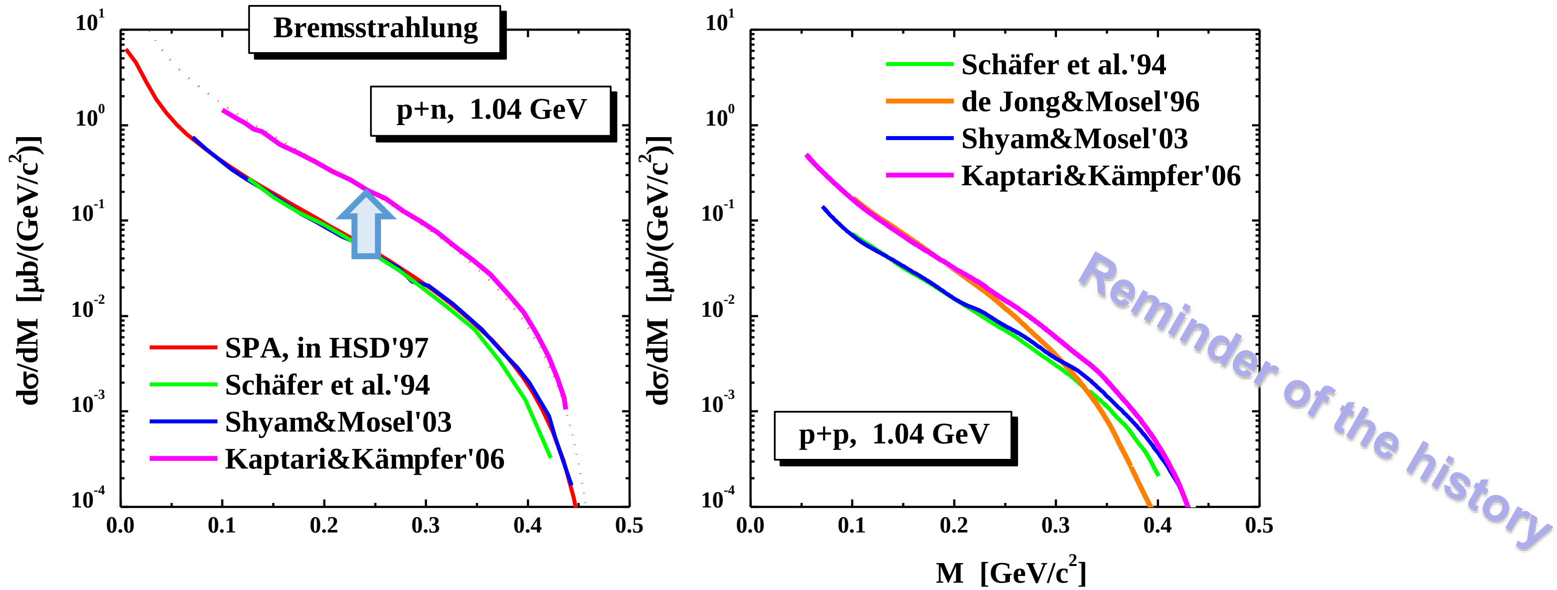

New OBE-model (Kaptari&Kämpfer, NPA 764 (2006) 338):

- **pn bremsstrahlung is larger by a factor of 4 than it has been calculated before (and used in transport calculations)!**
- **pp bremstrahlung is smaller than pn, however, not zero; consistent with the 1996 calculations from de Jong in a T-matrix approach**

2007 (era of HADES): The DLS puzzle is solved by accounting for a larger pn bremsstrahlung !!!

E.B., W. Cassing, Nucl.Phys.A 807 (2008) 214-250, 0712.0635 [nucl-th]

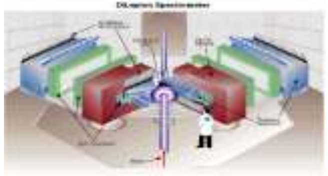

HSD: Dileptons from p+p, p+d, A+A - DLS

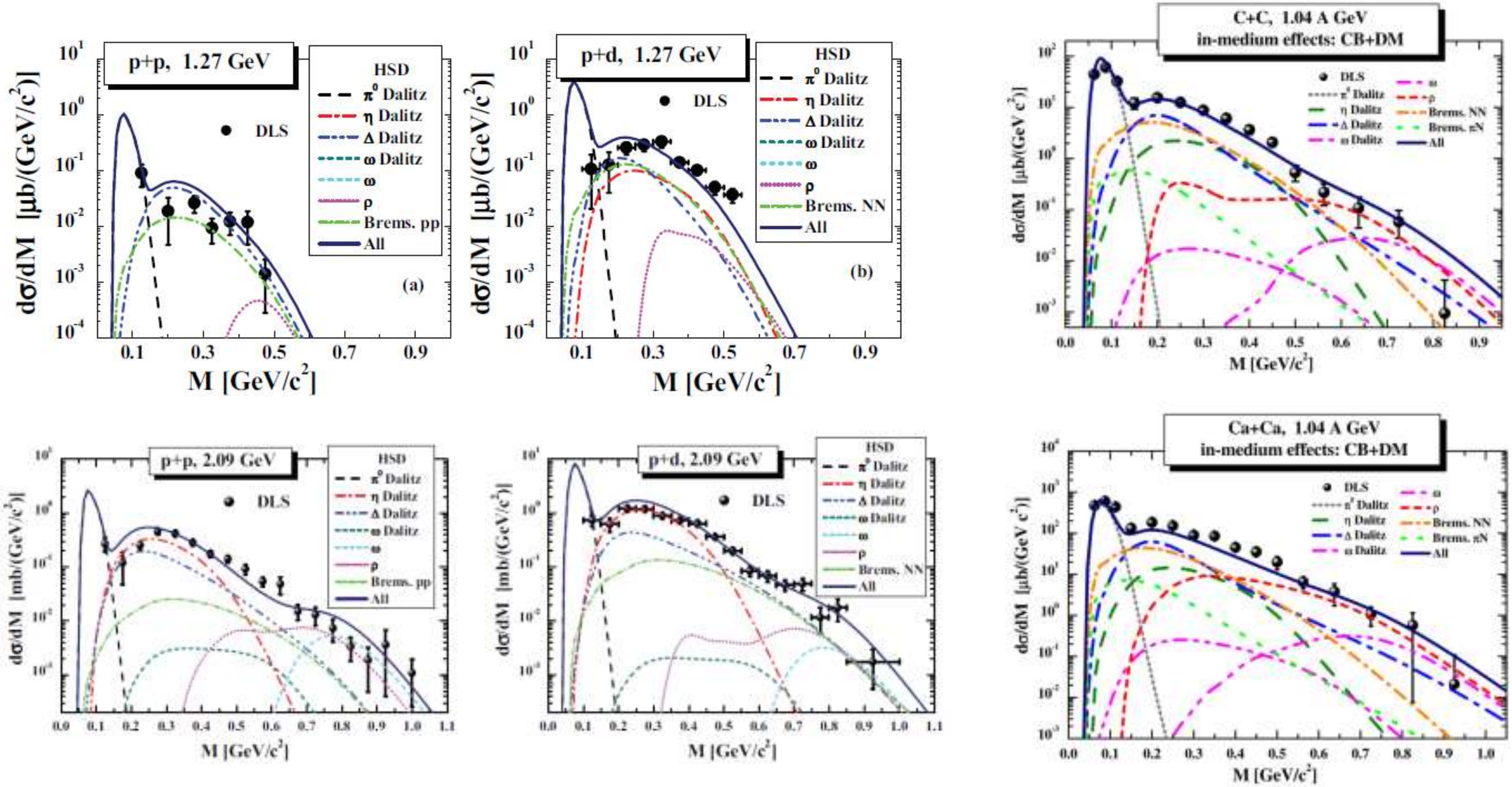

- **bremsstrahlung** and Δ-Dalitz are the dominant contributions in A+A for 0.15 < M < 0.55 GeV at 1 A GeV !

E.B., W. Cassing, Nucl.Phys.A 807 (2008) 214-250, 0712.0635 [nucl-th]

HSD: Dileptons from p+p, p+n and p+d - HADES

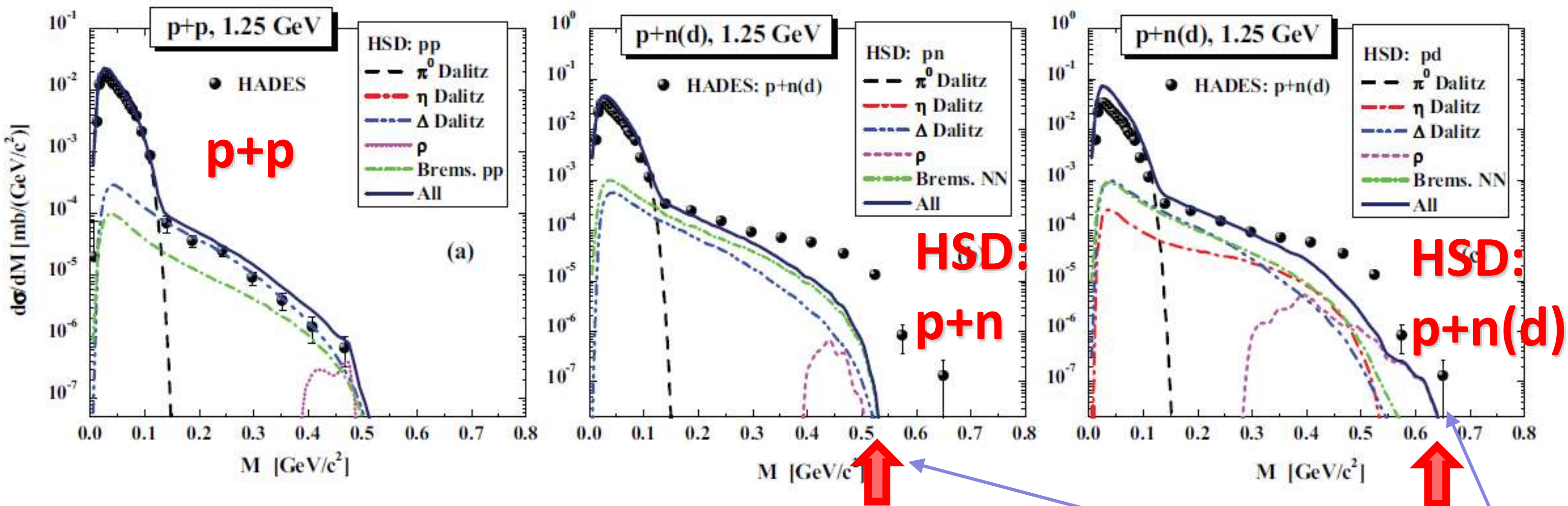

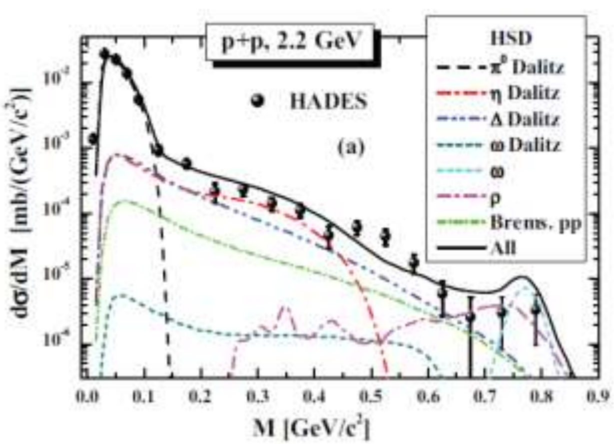

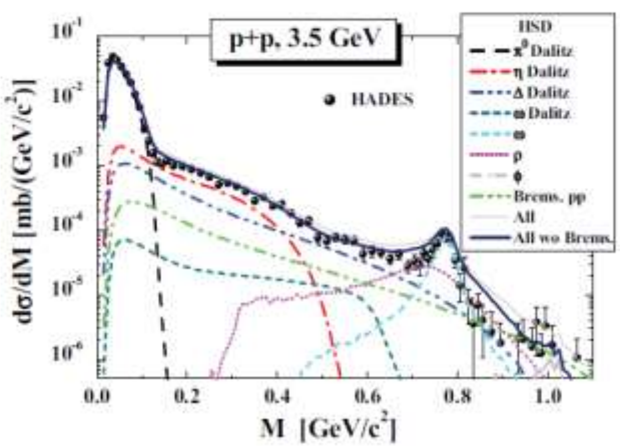

- Big influence of the Fermi-motion in p+n(d)
- shift of M_{max} compared to the ‚true‘ p+n

- New exp. data on p+n are needed! → SPD/NICA

E.B., J. Aichelin, M. Thomere, S. Vogel, and M. Bleicher, PRC 87 (2013) 064907

Dileptons at SIS energies - HADES

- **HADES: dilepton yield dN/dM scaled with the number of pions $N_{\pi 0}$**

- **Dominant hadronic sources at $M>m_\pi$:**
  - **η, Δ Dalitz decays**
  - **NN bremsstrahlung**
  - **direct ρ decay**

➢ **ρ meson = strongly interacting resonance**
strong collisional broadening of the ρ width

- **In-medium effects are more pronounced for heavy systems such as Ar+KCl than C+C**

- **The peak at M~0.78 GeV relates to ω/ρ mesons decaying in vacuum**

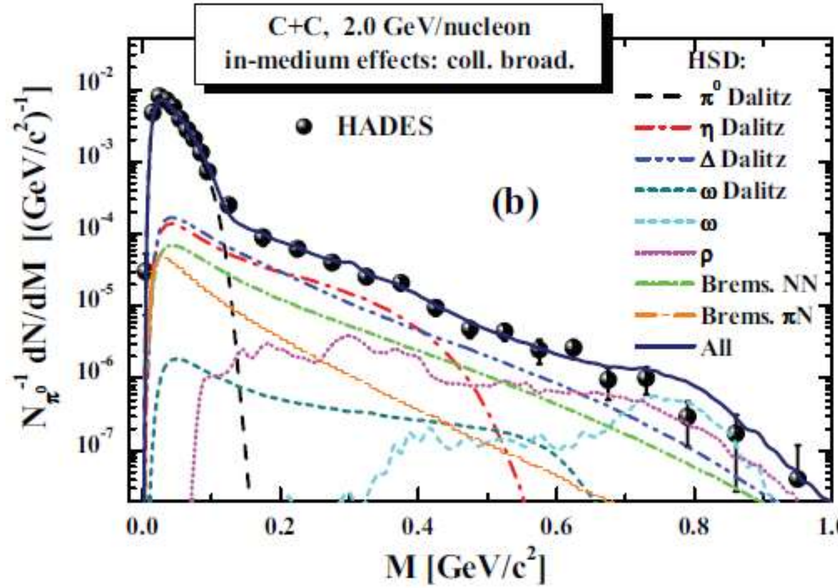

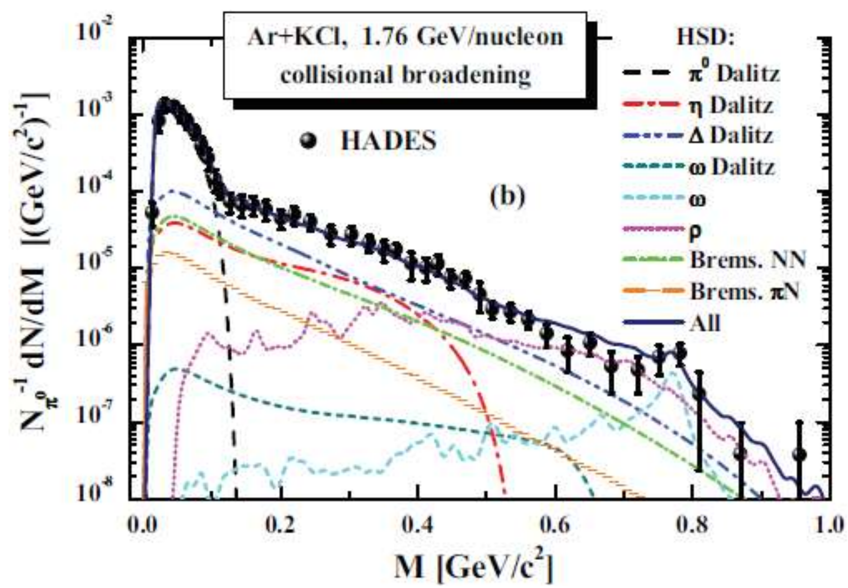

E.Bratkovskaya., J. Aichelin, M. Thomere, S. Vogel, and M. Bleicher, PRC 87 (2013) 064907

Dileptons at SIS (HADES): Au+Au

HADES, Nature Phys.15 (2019) 1040

HADES : Au+Au, 1.23 A GeV

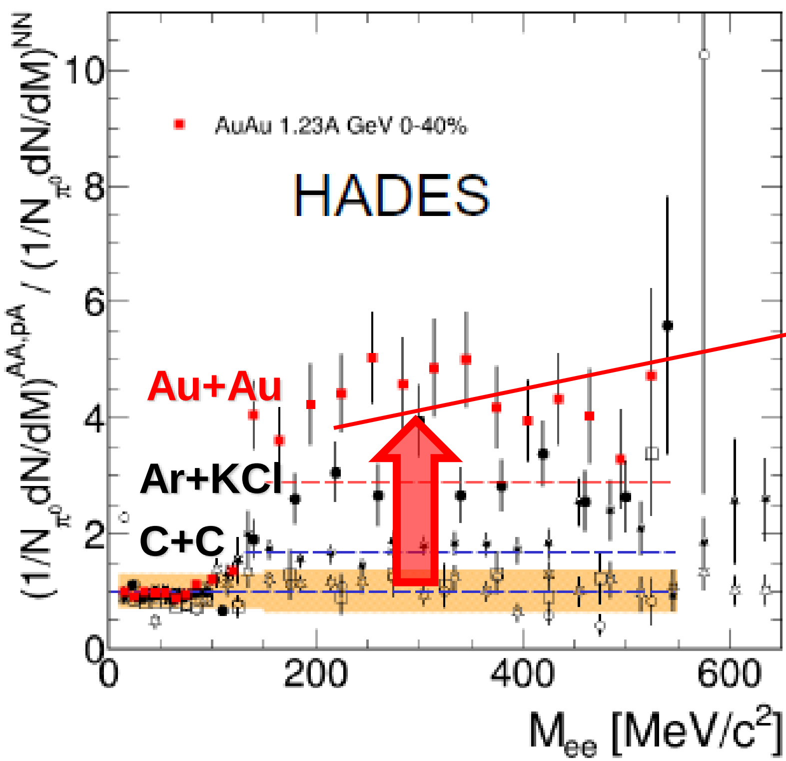

▪ **HSD predictions (2013)**

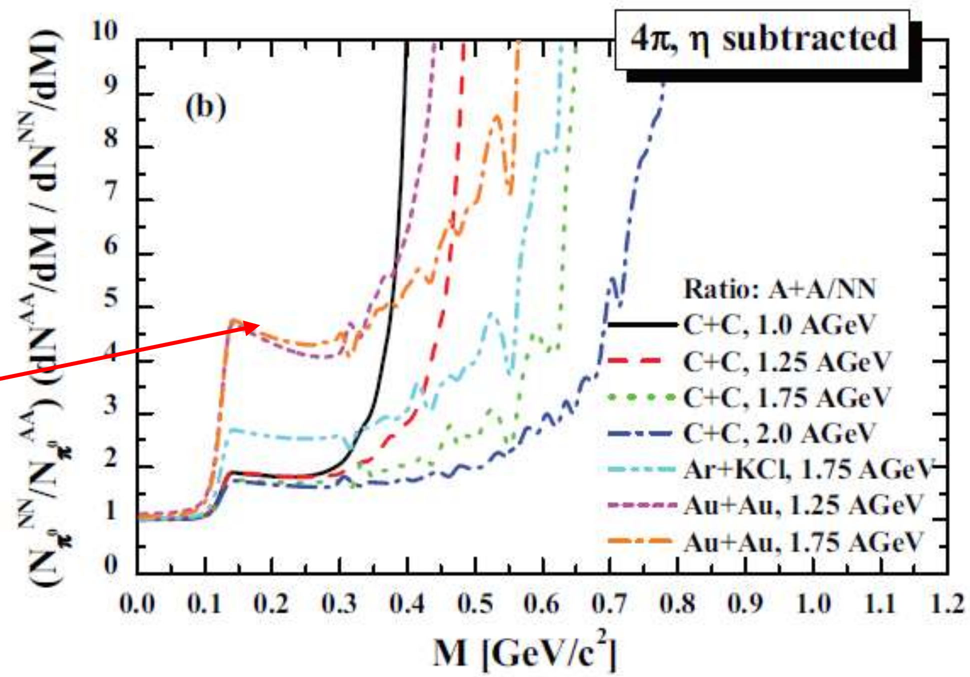

- ❑ **Strong in-medium enhancement** of dilepton yield in Au+Au vs. NN
- ❑ **Increases with the system size!**

1) the **multiple Δ regeneration** – dilepton emission from intermediate Δ's which are part of the reaction cycles Δ→πN; πN →Δ and NN→NΔ; NΔ→NN

2) the **pN bremsstrahlung** which scales with N_{bin} and not with N_{part} , i.e. pions;

E.B., J. Aichelin, M. Thomere, S. Vogel, M. Bleicher, PRC 87 (2013) 064907

Lessons from SPS: NA60

❑ **Dilepton invariant mass spectra:**

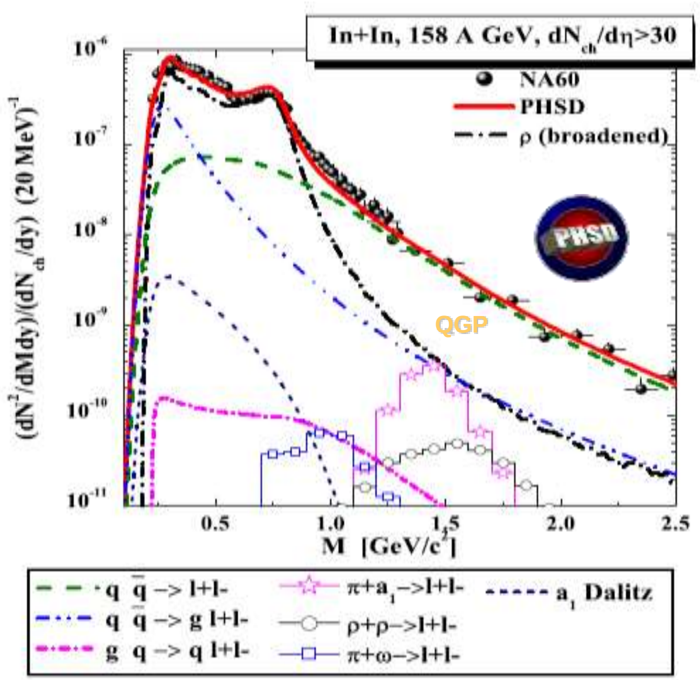

NA60: Eur. Phys. J. C 59 (2009) 607

❑ **Inverse slope parameter T_{eff}:**
spectrum from QGP is softer than from hadronic phase since the QGP emission occurs dominantly before the collective radial flow has developed

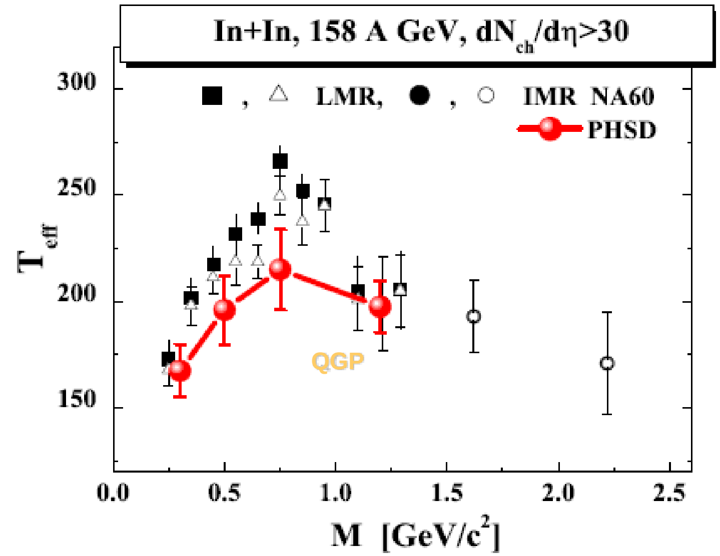

PHSD:
Linnyk et al, PRC 84 (2011) 054917

Message from SPS: (based on NA60 and CERES data)

1) **Low mass spectra** - evidence for the **in-medium broadening of ρ-mesons**
2) Intermediate mass **spectra above 1 GeV** - dominated by **partonic radiation**
3) The rise and fall of T_{eff} – evidence for the thermal **QGP radiation**
4) **Isotropic angular distribution** – indication for a **thermal origin of dimuons**

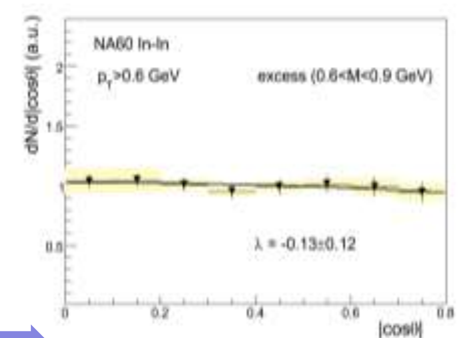

PRL 102 (2009) 222301

Dileptons: QGP vs charm

STAR BES data and the ALICE data are described by PHSD within a collisional broadening scenario for the vector meson spectral functions + QGP + correlated charm

Excitation function of dilepton yield integrated for 1.2<M<3GeV

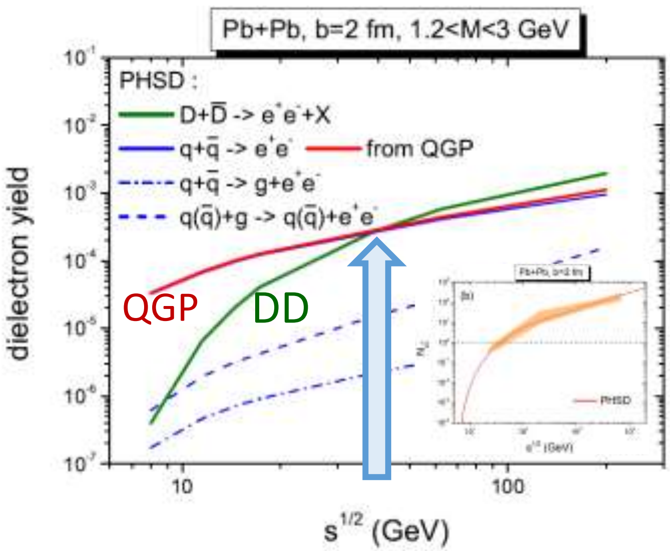

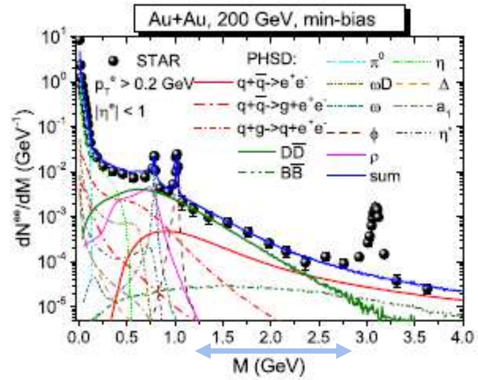

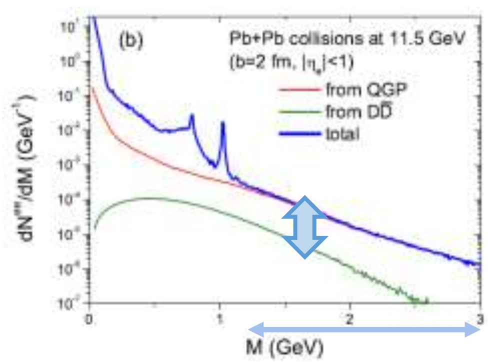

The inverse slope parameter of m_T spectra in the mass range M=[1.75,2.95]

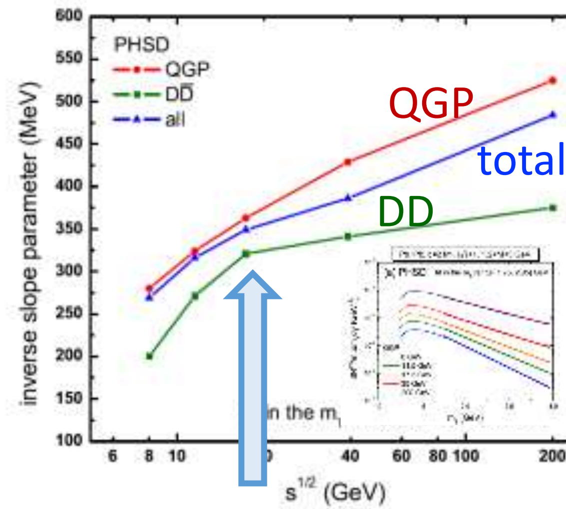

- **Dileptons from QGP overshine charm dileptons with decreasing beam energy!**
- **QGP contribution is harder than that from D-Dbar**

➔ **Good perspectives for FAIR/NICA and BES RHIC!**

T.Song, P. Moreau et al., Phys. Rev. C97 (2018), 064907; Phys. Rev. C98 (2018), 041901; Phys. Rev. D 98 (2018) 116007

Dilepton anisotropy coefficients

E.B., V.D. Toneev, O.V. Teryaev et al. **(Phys. Lett. B 348 (1995) 283 and 325 ; B 362 (1995) 17, B376 (1996) 12; Z. Phys. C75 (1997)197)**

dσ/d(cosθ) ~ 1 + B cos²θ

$$B = \frac{3\rho_{11} - 1}{1 - \rho_{11}}$$

$$\rho_{00} + 2\rho_{11} = 1$$

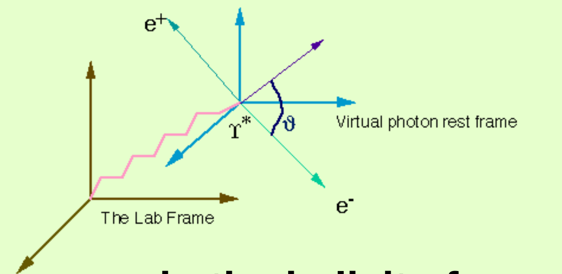

in the helicity frame

The Definition of the Theta_Decay angle

Anisotropy coefficients for elementary channels:

- **pseudoscalar mesons (e.g. π^0 and η):**
  B = +1
- **vector mesons (e,g, ρ, ω and ϕ) from NN→VX: if no preferred spin orientation of VM**
  B = 0
- **π π annihilation: $\pi^+\pi^- \to \rho \to e^+e^-$:**
  p wave (L=1 ⊥ to π π scattering plane)
  B = -1

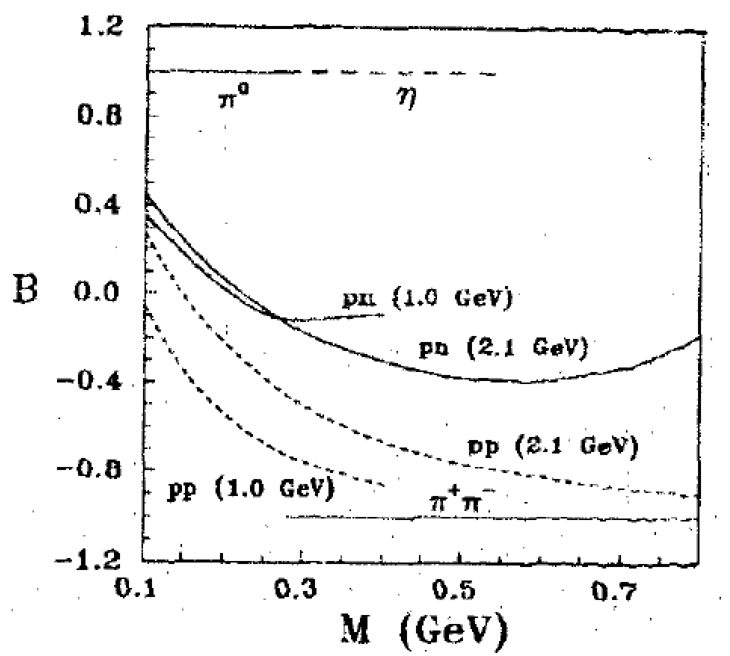

- **Δ and N* decays: B ≠ 0**

- **NN and πN bremsstrahlung: B ≠ 0**

Dilepton anisotropy coefficient

Total differential cross section for h+h (hadron+hadron or A+A) reaction:

$$\frac{d\sigma^{hh}}{dM\,d\cos\theta_{hh}} = \sum_{i=channel} \frac{d\sigma_i^{hh}}{dM\,d\cos\theta_{hh}} = A^{hh}(M)(1 + B^{hh}(M)\cos^2\theta_{hh})$$

$$B^{hh}(M) = \sum_{i=channel} < B_i^{hh}(M) >$$

The "weighted" anisotropy coefficients for "*i*" channel → to compare to exp. data which measure the sum of all contributions dσ/dM

$$< B_i^{hh}(M) >= \frac{\frac{d\sigma_i^{hh}}{dM} \cdot \frac{B_i^{hh}}{1+\frac{1}{3}B_i^{hh}}}{\sum_i \frac{d\sigma_i^{hh}}{dM} \cdot \frac{1}{1+\frac{1}{3}B_i^{hh}}}$$

$$S_i(M,\theta) \equiv \frac{d\sigma_i}{dM\;d\cos\theta}$$

$$B_i = \frac{S_i(M,\theta=0^o)}{S_i(M,\theta=90^o)} - 1$$

Dilepton anisotropy coefficient

B **from** **Δ-decay and Bremsstrahlung**
("pn" on plots):
sensitive to the model details:
B **from SPA <** ***B*** **from OBE model**

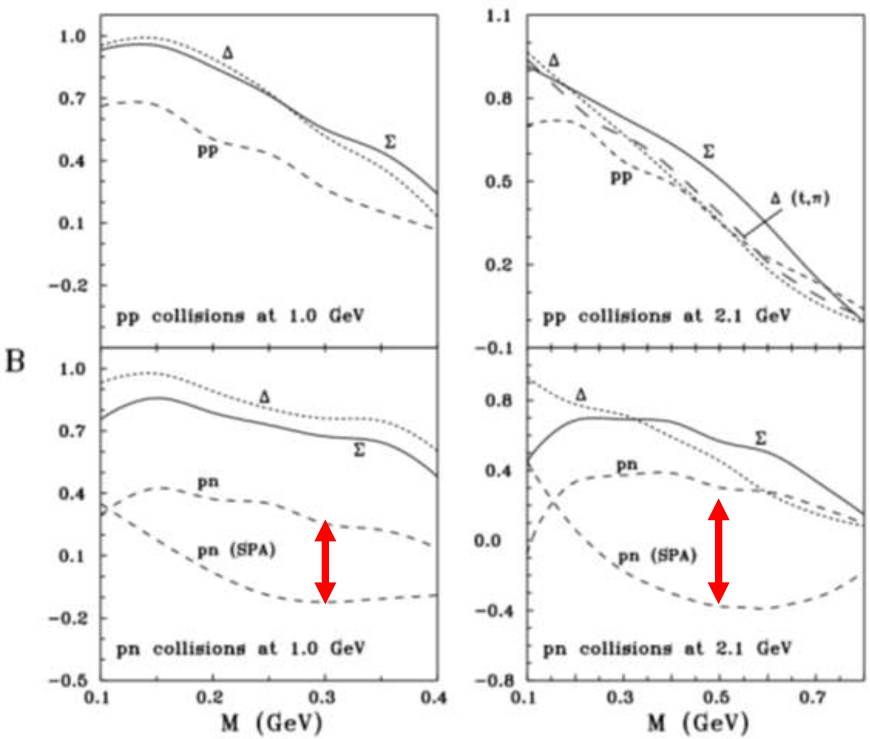

The "weighted" anisotropy coefficients for p+p, p+n and p+d collisions

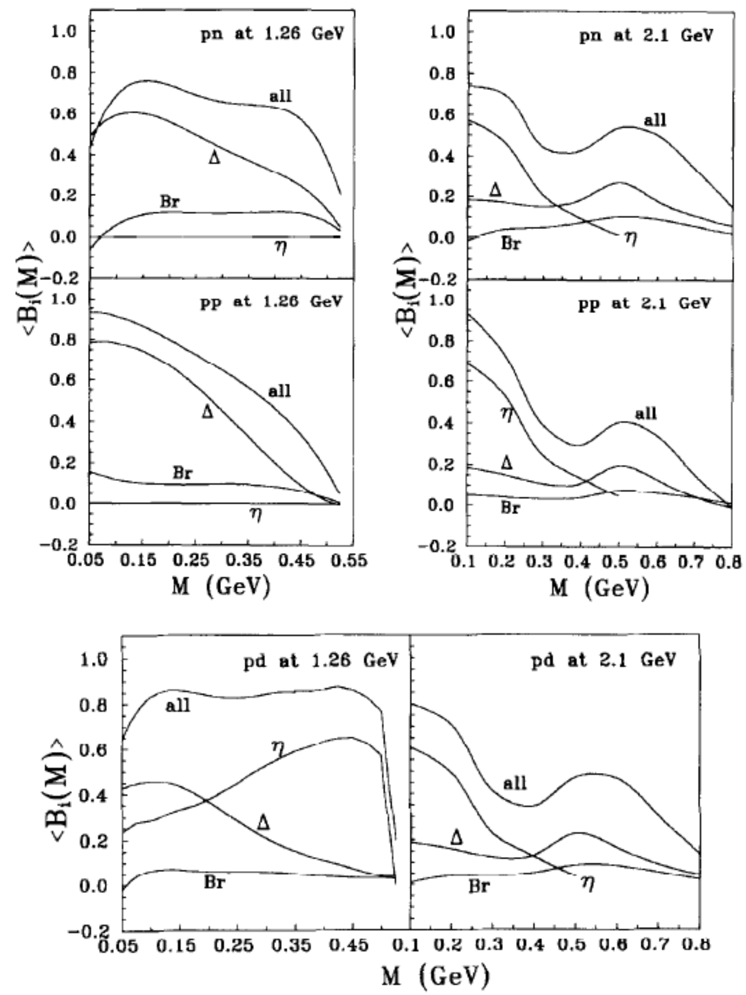

Dilepton anisotropy coefficient

The **"weighted" anisotropy coefficients** for p+Be and A+A collisions

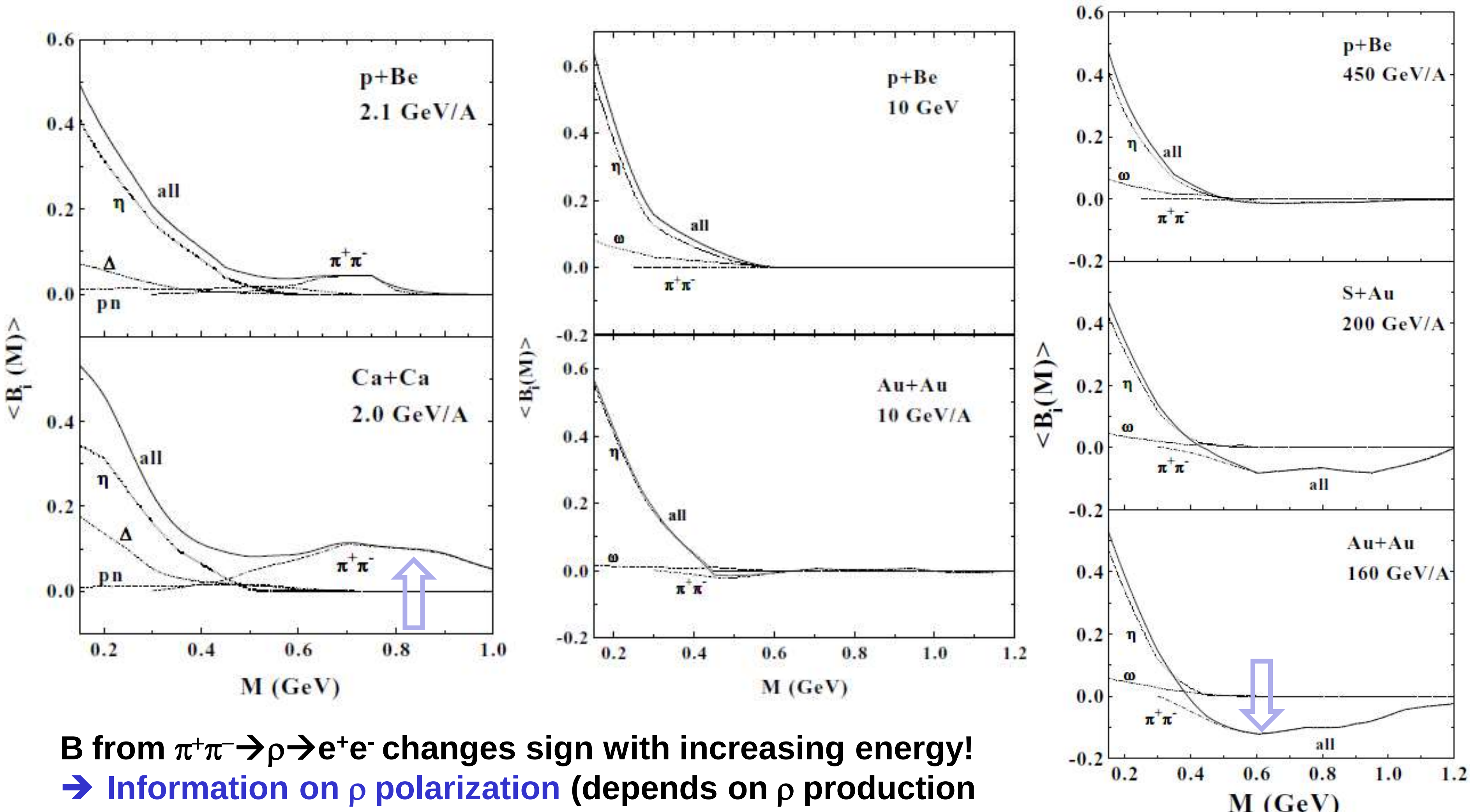

B from $\pi^+\pi^- \rightarrow \rho \rightarrow e^+e^-$ changes sign with increasing energy!

➔ **Information on ρ polarization** (depends on ρ production mechanism)!

➔ **Opportunities for the SPD dilepton program!**

Influence of the electromagnetic fields on p+A and A+A dynamics

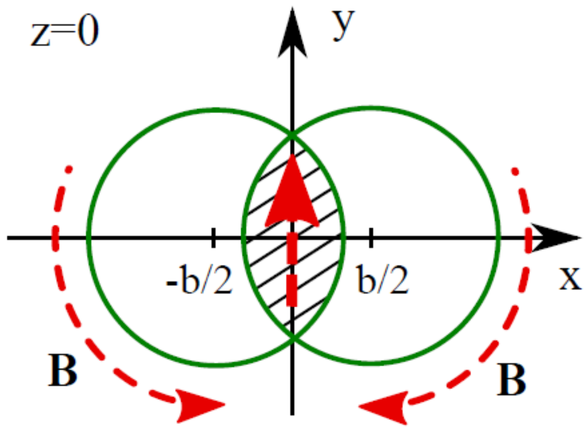

PHSD with electromagnetic fields

Generalized transport equations in the presence of electromagnetic fields :

$$\dot{\vec{r}} \rightarrow \frac{\vec{p}}{p_0} + \vec{\nabla}_p U \,, \qquad U \sim Re(\Sigma^{ret})/2p_0$$

$$\dot{\vec{p}} \rightarrow -\vec{\nabla}_r U + e\vec{E} + e\vec{v} \times \vec{B}$$

$$\begin{cases} \vec{B} = \vec{\nabla} \times \vec{A} \\ \vec{E} = -\vec{\nabla}\Phi - \frac{\partial \vec{A}}{\partial t} \end{cases}$$

$$\vec{A}(\vec{r},t) = \frac{1}{4\pi} \int \frac{\vec{j}(\vec{r'},t')\, \delta(t - t' - |\vec{r} - \vec{r'}|/c)}{|\vec{r} - \vec{r'}|} d^3r'dt'$$

$$\Phi(\vec{r},t) = \frac{1}{4\pi} \int \frac{\rho(\vec{r'},t')\, \delta(t - t' - |\vec{r} - \vec{r'}|/c)}{|\vec{r} - \vec{r'}|} d^3r'dt'$$

- **Magnetic field evolution in HSD/PHSD :**

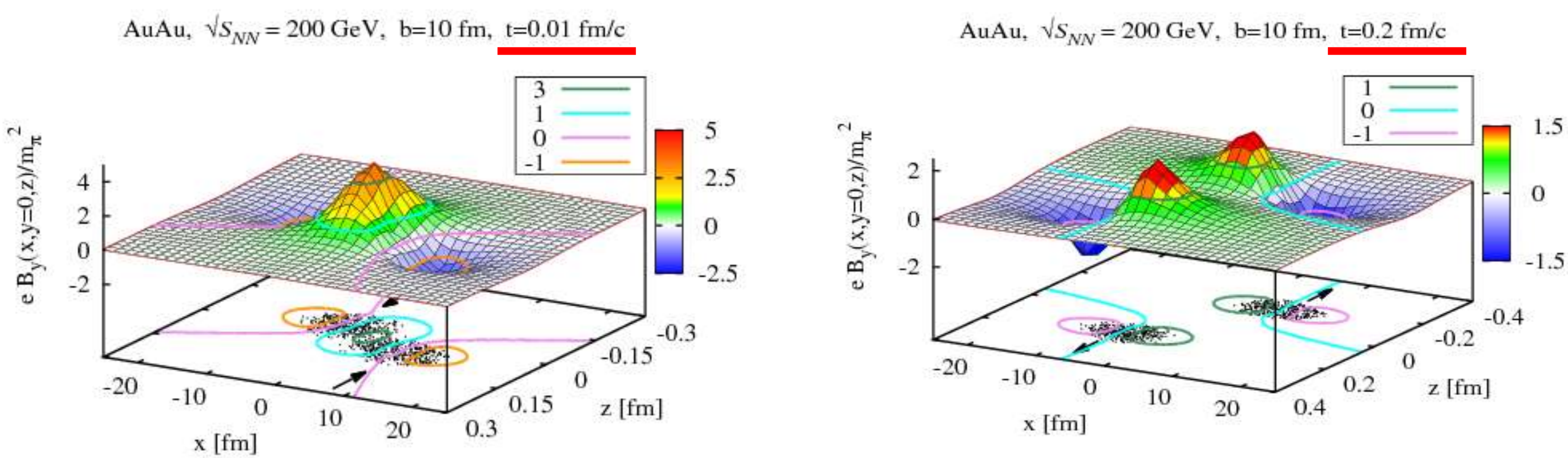

V. Voronyuk, V.D. Toneev et al., Phys.Rev. C83 (2011) 054911

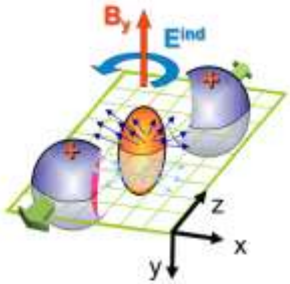

Time dependence of eB_y

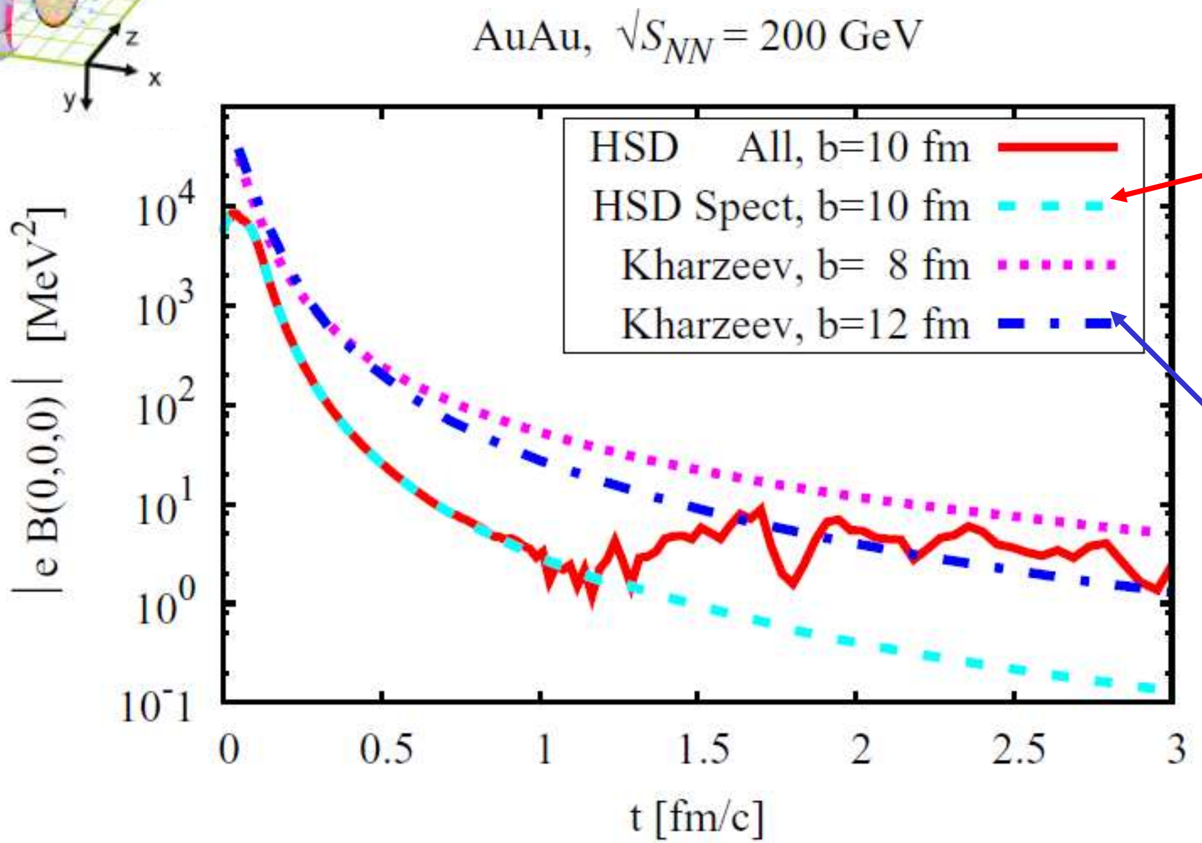

HSD: V.Voronyuk, et al., PRC83 (2011) 054911

Collision of two infinitely thin layers (pancake-like)
D.E. Kharzeev et al., NPA803, 227 (2008)

- **Until t~1 fm/c the induced magnetic field is defined by spectators only**
- **Maximal magnetic field is reached during nuclear overlap time Δt~0.2 fm/c, then the field goes down exponentially**

V. Voronyuk, V.D. Toneev et al., Phys.Rev. C83 (2011) 054911

Angular correlation w.r.t. reaction plane

$$\langle \cos(\psi_\alpha + \psi_\beta - 2\Psi_{RP}) \rangle$$

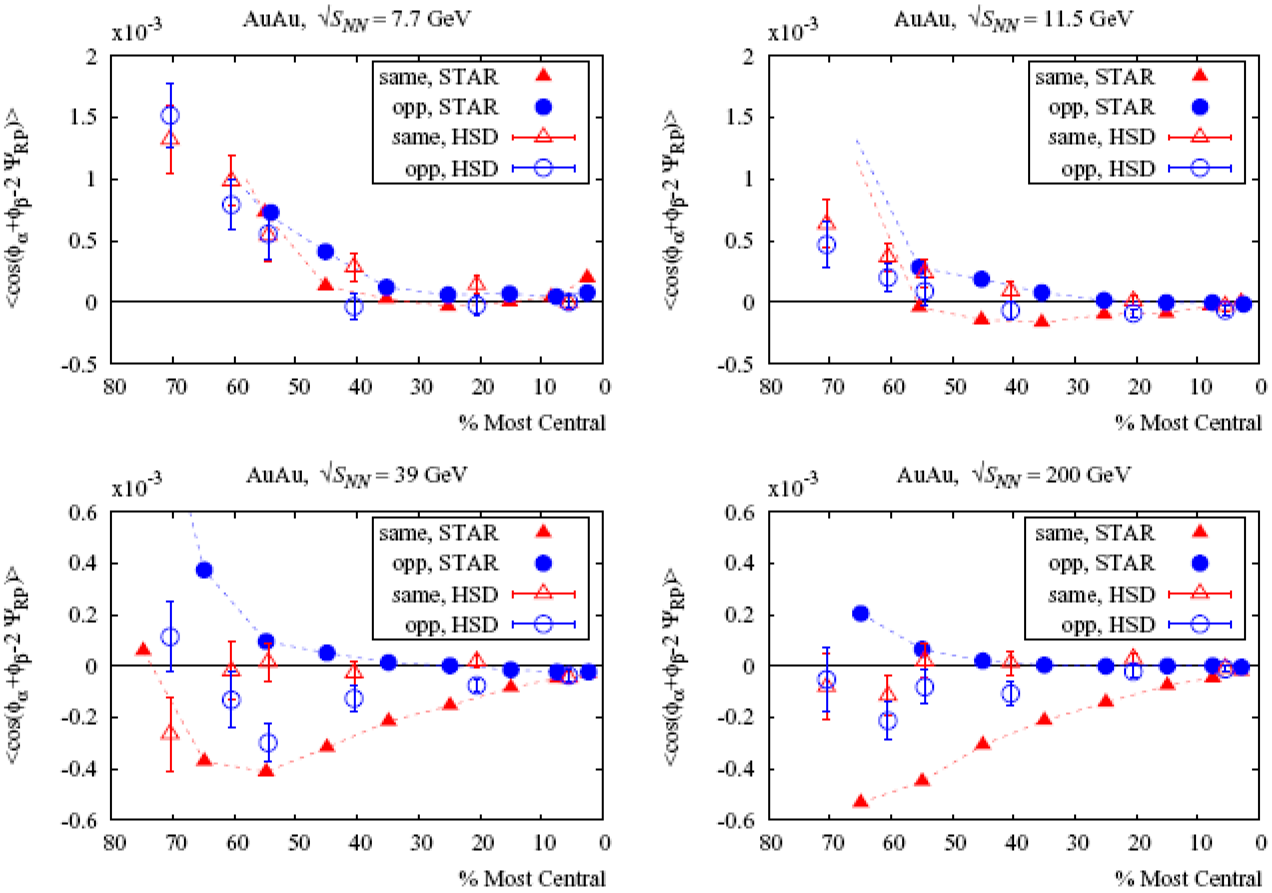

Angular correlation is of hadronic origin up to sqrt(s) = 11 GeV !

V. D. Toneev, V. Voronyuk et al., PRC 85 (2012) 034910

Electromagnetic fields: A+A vs p+A

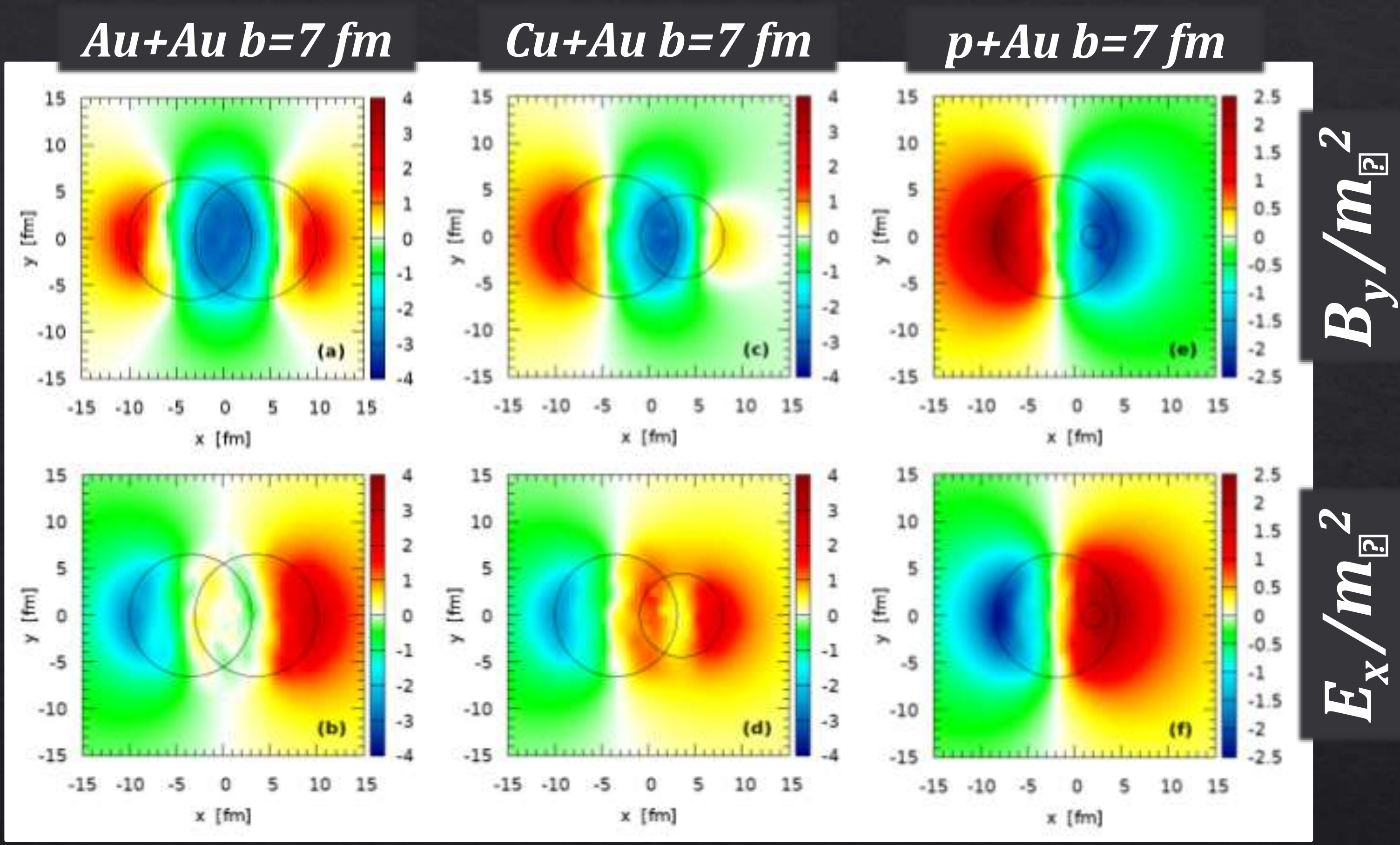

initial transvese profiles at RHIC 200 GeV

intense electric fields directed from the heavy nuclei to light one in the overlap region of asymmetric colliding systems due to the different number of protons in the two nuclei

Voronyuk, Toneev, Voloshin and Cassing, Phys. Rev. C 90, 064903 (2014)
Oliva, Moreau, Voronyuk and Bratkovskaya, Phys. Rev. C 101, 014917 (2020)

EMF effect on directed flow in asymmetric systems

Cu+Au collisions at 200 GeV

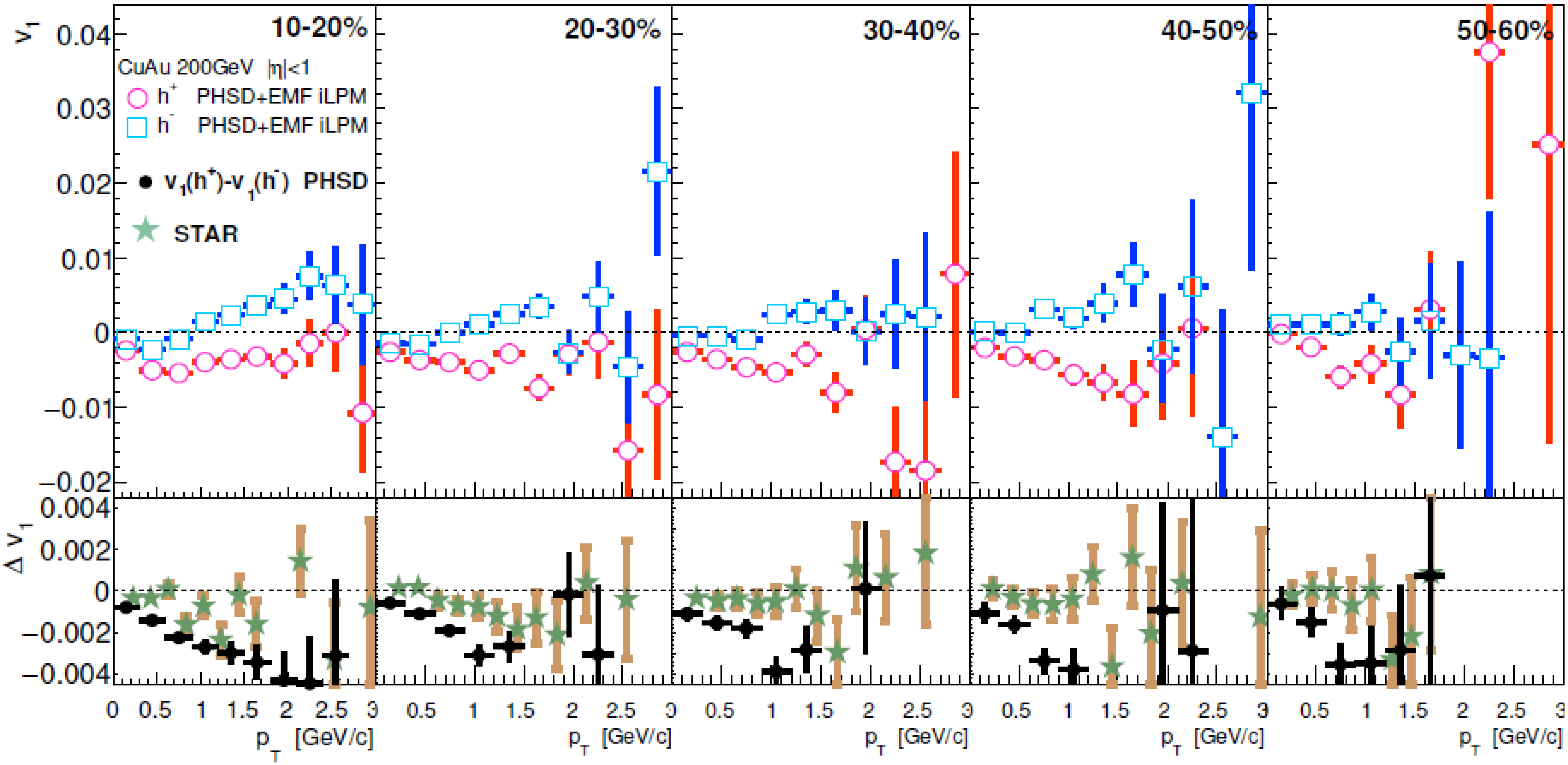

There is splitting of v_1 of negative and positive hadrons in EMF for asymmetric HICs!

V.D. Toneev, V. Voronyuk, E.E. Kolomeitsev, W. Cassing, Phys. Rev. C95, 034911 (2017)

EMF and directed flow in p+A

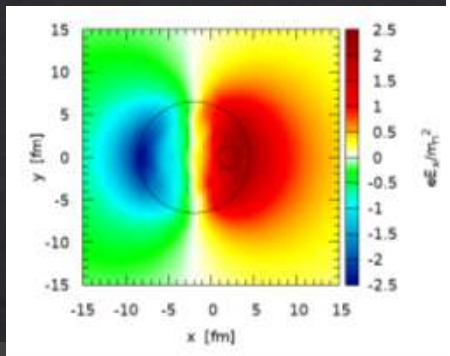

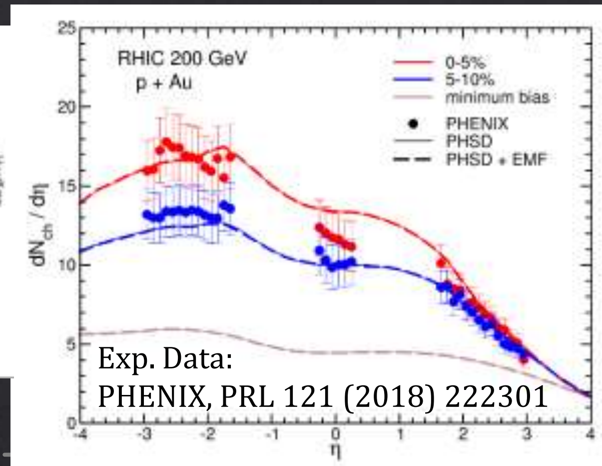

Asymmetry in charged particle and electric field profiles in p+Au

- enhanced particle production in the Au-going direction
- electric field directed from the heavy ion to the proton

Oliva, Moreau, Voronyuk and Bratkovskaya, Phys. Rev. C 101, 014917 (2020)

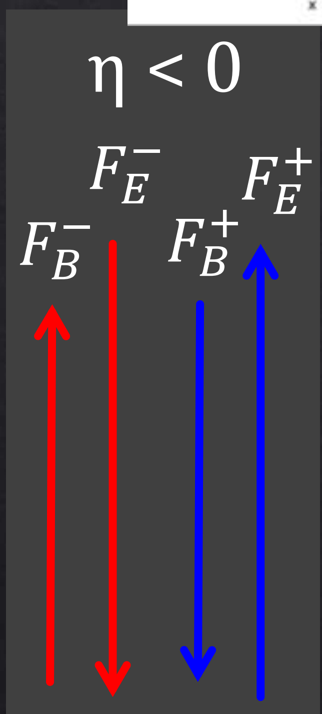

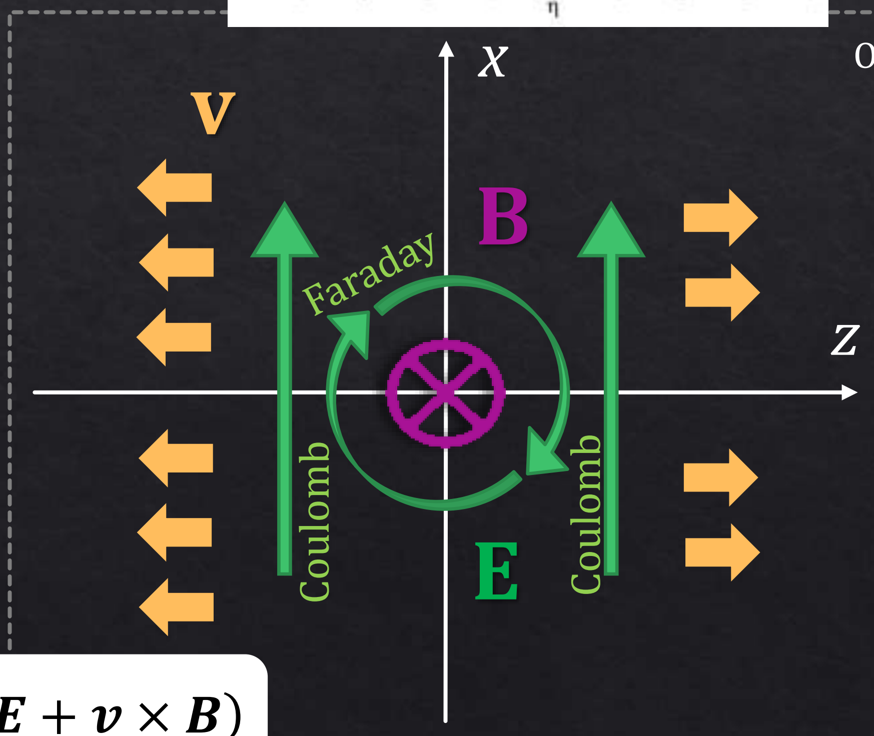

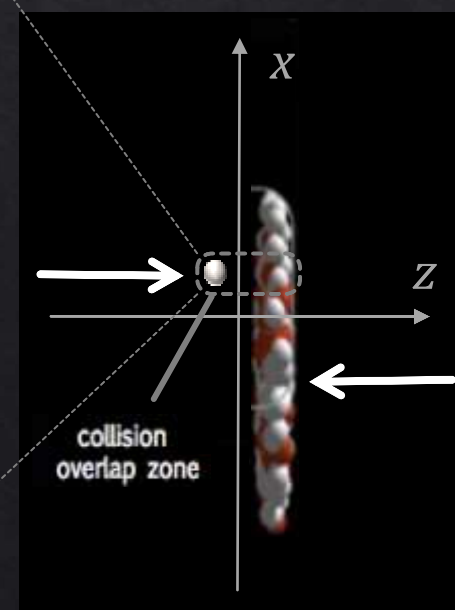

$$\boldsymbol{F}_{\boldsymbol{Lorentz}} = q(\boldsymbol{E} + \boldsymbol{v} \times \boldsymbol{B})$$

EMF and directed flow in p+A

rapidity dependence of the
DIRECTED FLOW OF PIONS

$$v_1(y) = \langle \cos[\varphi(y)] \rangle$$

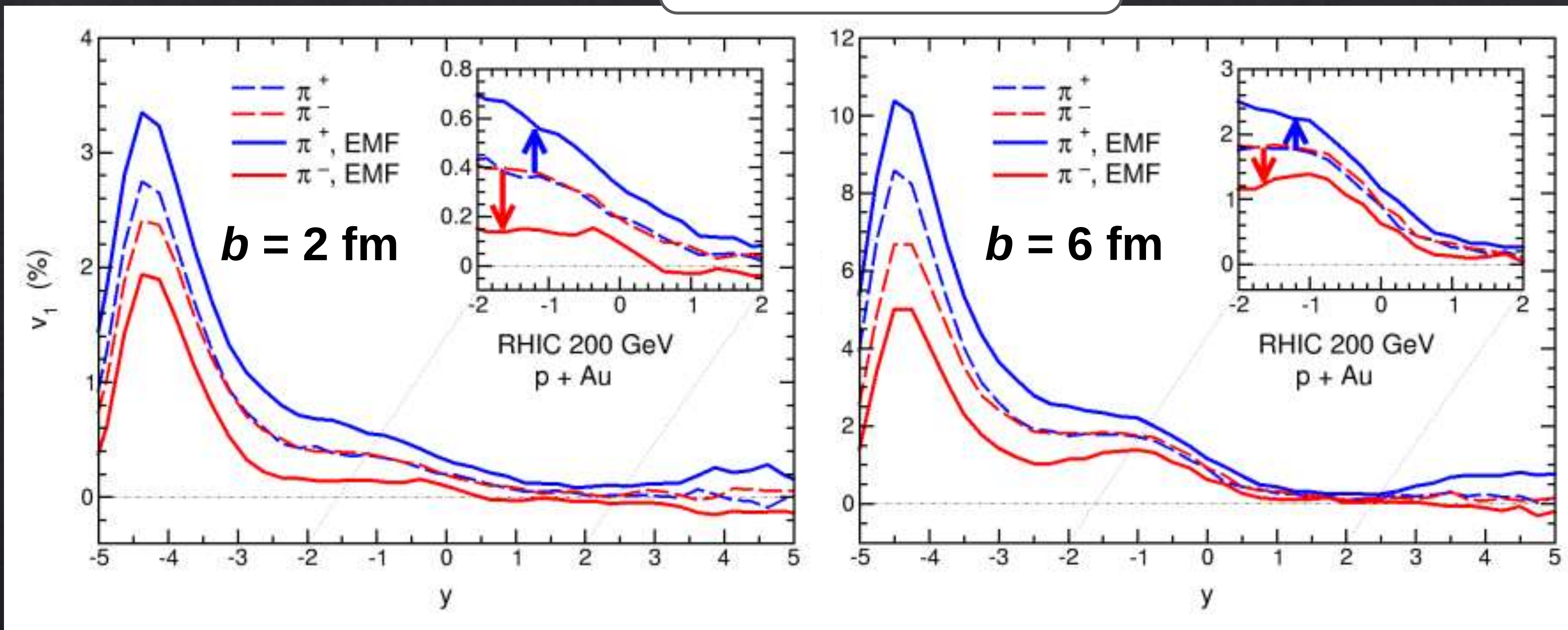

Oliva, Moreau, Voronyuk and Bratkovskaya, Phys. Rev. C 101, 014917 (2020)

Splitting of π^+ and π^- induced by the electromagnetic field

EMF and directed flow in p+A

rapidity dependence of the
DIRECTED FLOW OF KAONS

$$v_1(y) = \langle \cos[\varphi(y)] \rangle$$

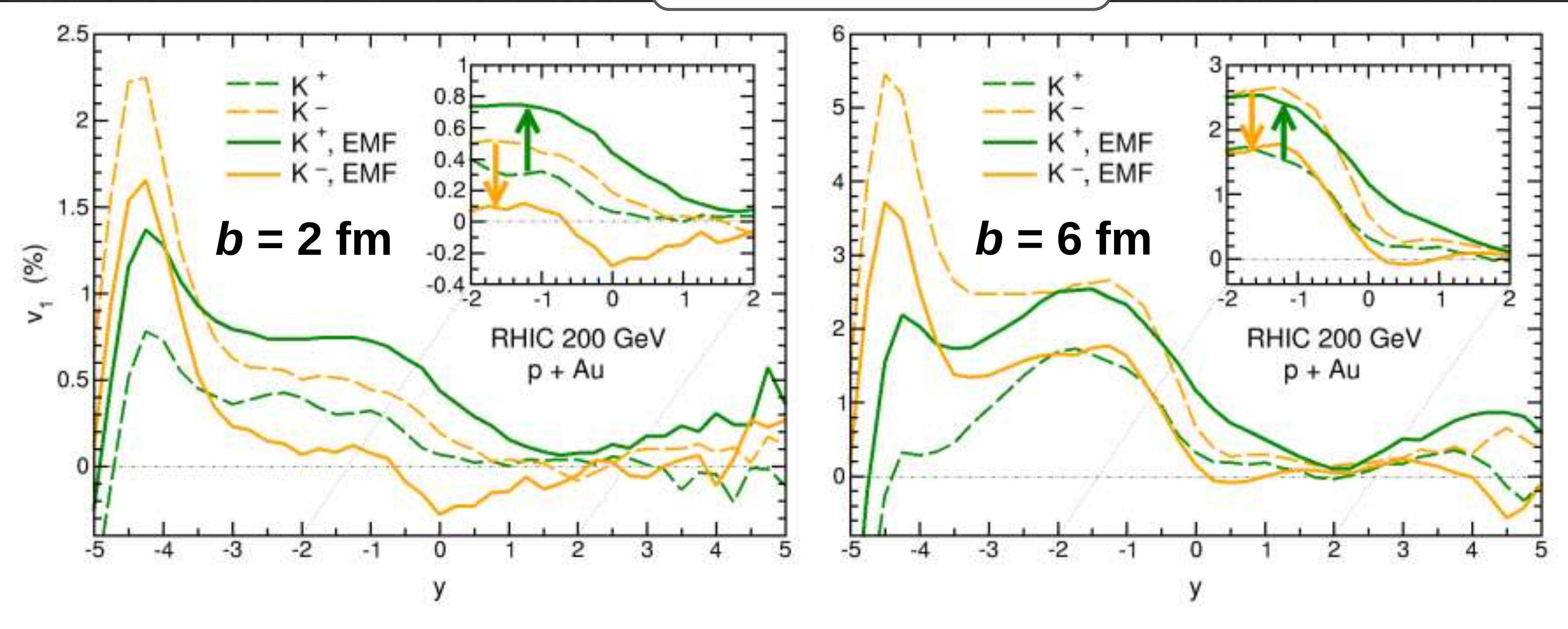

Oliva, Moreau, Voronyuk and Bratkovskaya, Phys. Rev. C 101, 014917 (2020)

Splitting of K^+ and K^- induced by the electromagnetic field

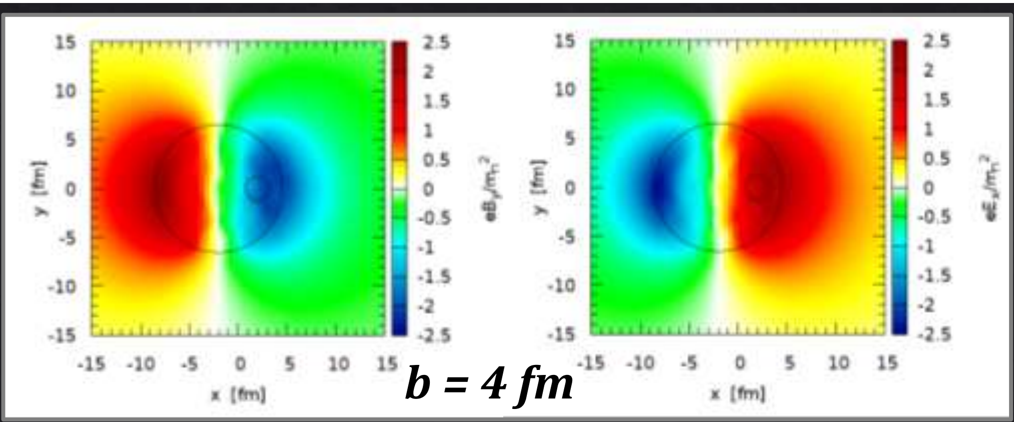

Elementary p+p, p+n reactions: PHSD “tune” of LUND model (PYTHIA, FRITIOF)

V. Kireyeu, I. Grishmanovskii, V. Kolesnikov, V. Voronyuk, and E. B.,
Eur.Phys.J.A 56 (2020) 223; e-Print:2006.14739 [hep-ph]

Elementary reactions p+p, p+n, n+n

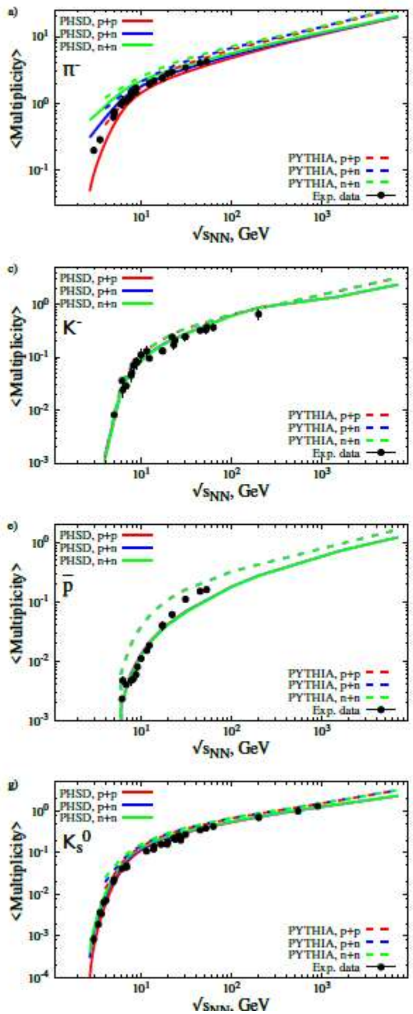

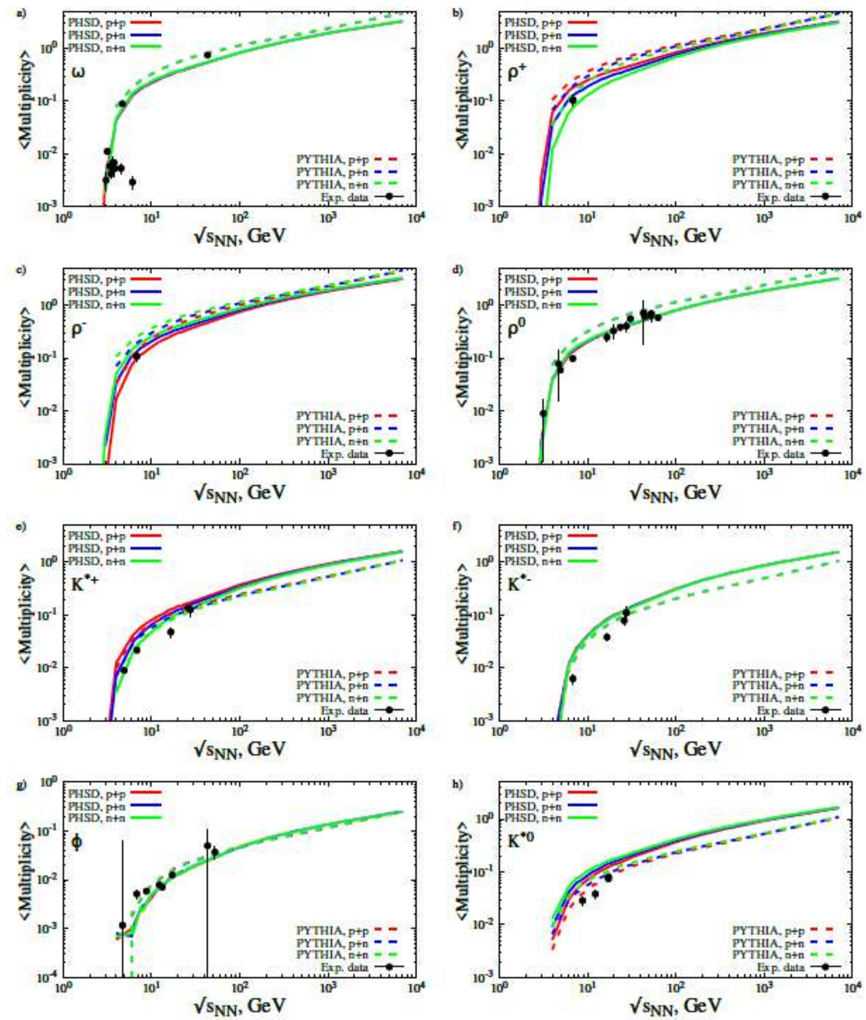

- Existing experimental data on p+p are pure!
  Practically NO data on p+n reactions!

V. Kireyeu et al., Eur.Phys.J.A 56 (2020) 223

➔ NICA/SPD can improve the situation!

SPD (NICA) :

measurements for p+p, p+A, A+A

➔ can provide an important information for the particle and heavy-ion physics!

Thank you for your attention !